

Stony Brook University



OFFICIAL COPY

The official electronic file of this thesis or dissertation is maintained by the University Libraries on behalf of The Graduate School at Stony Brook University.

© All Rights Reserved by Author.

Correlations in Low-Dimensional Systems

A Dissertation Presented

by

Sebastian Andres Reyes

to

The Graduate School

in Partial Fulfillment of the Requirements

for the Degree of

Doctor of Philosophy

in

Physics

Stony Brook University

August 2007

Stony Brook University

The Graduate School

Sebastian Andres Reyes

We, the dissertation committee for the above candidate for the Doctor of Philosophy degree, hereby recommend acceptance of this dissertation.

Alexei M. Tselik – Dissertation Advisor
Professor, Department of Physics and Astronomy

Adam Durst – Chairperson of Defense
Professor, Department of Physics and Astronomy

Dominik Schneble
Professor, Department of Physics and Astronomy

Robert Konik
Associate Scientist
Brookhaven National Laboratory

This dissertation is accepted by the Graduate School.

Lawrence Martin
Dean of the Graduate School

Abstract of the Dissertation
Correlations in Low-Dimensional Systems

by

Sebastian Andres Reyes

Doctor of Philosophy

in

Physics

Stony Brook University

2007

We examine three different low dimensional condensed matter systems.

Chapter 2 is concerned with the one dimensional quantum Ising model in a transverse magnetic field. Using exact results for the correlators of the classical two dimensional Ising model we show how to obtain two point correlators of the order parameter field for two different regimes.

In the third chapter we study the problem of two spin-1/2 Heisenberg chains interacting at a single point. Using equivalences between different models we show that the correlators of the physical

fields have non-universal exponents.

Finally, in Chapter 4 we explore the possibility of spin density wave (SDW) formation in graphene (two dimensional layers of graphite) that may be facilitated by the application of a magnetic field in the direction of the plane of the graphene sheet. We find an order parameter that combines sublattice, valley and spin degrees of freedom. Due to reduced dimensionality, we pay special attention to critical fluctuations.

To Javiera.

Contents

List of Figures	viii
Acknowledgements	x
1 Introduction	1
1.1 One-dimensional Systems	2
1.2 Two-dimensional Systems	4
2 Order Parameter Correlators of the Quantum Ising Model	7
2.1 Basics of the Ising Model	8
2.1.1 Correspondence between 2D classical and 1D quantum Ising models	12
2.2 Finite temperature correlation function: the virial expansion .	15
2.2.1 Introduction	15
2.2.2 Two-point Correlators	17
2.2.3 Results and Conclusions	22
2.3 High Temperature Limit of the Order Parameter Correlation Function	26
2.3.1 Introduction	26
2.3.2 Quantum limit of the correlation functions	27
2.3.3 Real time asymptotics.	31
2.3.4 Conclusions	34
3 Crossed Spin-1/2 Heisenberg Chains as a Quantum Impurity Problem	35
3.1 Introduction	35
3.2 The Model: two Heisenberg chains interacting at a single point	37
3.3 Correlators for Staggered Magnetization	42

4	Spin Density Wave Formation in Graphene Facilitated by in-plane Magnetic Field	46
4.1	Introduction	47
4.1.1	Basics of Graphene	47
4.1.2	Density Wave Formation and in-plane Magnetic Field .	51
4.2	Mean Field Hamiltonian	53
4.2.1	Order Parameter Field	55
4.3	Effective Interaction and Mean Field Critical Temperature . .	57
4.4	Critical Fluctuations	60
4.5	Conclusions	65
5	General Conclusions	67
A	Matsubara Time Formalism	72
B	Transformation of sum (2.67) into a contour integral	74
C	Bosonization of the Heisenberg chain	80
D	Transformation of two Heisenberg chains into Majorana fermions	85
E	Calculation of Stiffness (ρ) for Ginzburg-Landau Theory (4.30)	89
	Bibliography	98

List of Figures

2.1	Phase diagram for the one dimensional quantum Ising model. There are three distinct low temperature regimes ($T \ll J$), in all of which Lorentz symmetry emerges and a field theory description is appropriate. In the <i>Lattice High T</i> ($T \gg J$) both Lorentz symmetry and universality are lost.	11
2.2	Critical line of the two dimensional classical Ising model. Above the line the system is in its ordered phase. When $\lambda < 1$ we are below the line and the system is in a paramagnetic state. . .	13
2.3	A graphic representation of Eq.(2.22). The ellipses are formfactors of σ operator. Lines with left arrows are $f^{(+)}(\theta) \exp[i\epsilon(\theta) + i\chi p(\theta)]$, lines with the right arrows are $f^{(-)}(\theta) \exp[-i\epsilon(\theta) - i\chi p(\theta)]$	18
3.1	Pictorial depiction of Hamiltonian 3.1. Heisenberg chains consist of spins (arrows) located at each site that interact with its nearest neighbor via exchange interaction. Additionally, there is also interaction between chains at a single site located at $x = 0$	37
4.1	Graphene's hexagonal lattice. Carbon atoms are arranged into two overlapping triangular lattices (u and v). We consider nearest neighbor hopping amplitude t	48
4.2	The spectrum of quasiparticles (4.2) as obtained from the nearest neighbor hopping Hamiltonian. Valence and conduction bands touch at two points inside the Brillouin zone. The low energy part of the spectrum consists of two cones separated by the vector $2\mathbf{Q}$	49
4.3	Graphene bands split by the in-plane magnetic field.	52
4.4	The spectrum of quasiparticles below the mean field critical temperature (4.11). A gap opens all around the Fermi surface located at $v \mathbf{k} = B$	54
4.5	Renormalization group flow of g for a bare value of $g_0 \approx 6.9$. g becomes lower than 1 only if $B \leq 10^{-3}K$	59

4.6	The stiffness at zero temperature ($\rho(0)$) is much larger than the mean field critical temperature (T_{MF}) at which the stiffness vanishes. Equation (4.37) is thus solved at a temperature close to T_{MF}	64
4.7	Schematic view of expected neutron scattering Bragg peaks. Peaks are located at wavevectors $\mathbf{0}$ and $\pm 2\mathbf{Q}$. The width of the peaks is given by the inverse correlation length of the $O(4)$ non-linear sigma model (4.40).	65
B.1	The figure shows the integration contours in the α plane. The circles are the poles of F at α_j given by (B.6).	77

Acknowledgements

I would like to take this opportunity to thank several people that made this thesis possible.

First, I would like to express my thanks to my thesis advisor, Alexei Tsvelik. I greatly benefited from his teachings during my years as his student. His extensive and deep knowledge of physics, together with his patience and generosity, made him a perfect mentor. I am deeply grateful for his time and dedication. Without him this thesis would certainly not have been possible.

During my time as a graduate student I also benefited from discussions and advice from other experienced researchers. I would like to mention in particular Alexander Abanov, Igor Aleiner and Robert Konik.

I would also like to thank my parents and my friends for their support during my time at Stony Brook. Knowing that I could always count on them was very important for me during these years.

Last, but certainly not least, I thank my wife, Javiera. Her continued love and support during the past few years made this work possible. This thesis is dedicated to her.

This research was supported by US DOE under contract number DE-AC02-98 CH 10886.

Publications

The present thesis is based on the following publications.

1.- **“Crossed Spin-1/2 Heisenberg Chains as a Quantum Impurity Problem”** (with A. M. Tsvelik) Phys. Rev. Lett. **95**, 186404 (2005). cond-mat/0507312

2.- **“High temperature limit of the order parameter correlation functions in the quantum Ising model”** (with A. M. Tsvelik) Nuclear Physics B **744**, 3, 330 (2006).

3.- **“Finite-temperature correlation function for the one-dimensional quantum Ising model: The virial expansion”** (with A. M. Tsvelik) Phys. Rev. B **73**, 220405(R) (2006). cond-mat/0605040

4.- **“Spin density wave in graphene facilitated by the in plane magnetic field”** (with A. M. Tsvelik and D. E. Kharzeev) cond-mat/0611251 (2006). (NOTE: several modifications to this manuscript, that are included in the present thesis, were later made with the additional collaboration of I. Aleiner.)

Chapter 1

Introduction

Dimensionality is one of the most defining properties of a physical system. In particular, since fluctuations always increase with a decrease of dimensionality, the latter most decisively affects properties of phase transitions. Fluctuations can preclude phase ordering such that ordered phases existing in three dimensions may not occur in lower dimensionality.

Strength of fluctuations in low-dimensional systems often makes it difficult a use of conventional theoretical tools such as mean field theory. At these circumstances one has to resort to more advanced methods such as bosonization and Bethe ansatz available in $(1+1)$ -dimensions (for quantum systems) and in two dimensions (for classical systems). Though these methods are very powerful their application to various problems, such as calculations of correlation functions, are frequently not quite straightforward and requires a considerable effort. In this thesis we address some of the problems of that kind.

1.1 One-dimensional Systems

One-dimensional systems exist in nature either directly or in their *quasi*-1D form as arrays of weakly coupled chains. In both cases they have also been the object of extensive experimental study in the last couple of decades when the advances in the synthesis made such systems available. Examples include the bulk materials consisting of well separated spin chains ($KCuF_3$) [2] or ladders ($SrCu_2O_3$) [3]. In such materials exchange interaction along the one-dimensional structure (chain or ladder) is much stronger than the interaction among them, resulting in quasi-one-dimensional behavior. There are a number of strictly one-dimensional systems such as, for example, carbon nanotubes, edge states in the quantum Hall effect or Josephson junction arrays, just to name a few.

It is worth mentioning that the increasing ability to produce higher magnetic fields and lower temperatures has also played a major role in the success of experimental studies in such materials.

From the point of view of the theorist, the study of one-dimensional systems is very appealing because of the fact that non-perturbative or even exact results can frequently be found. A very important analytical method to obtain such solutions is Bethe-ansatz. Introduced more than seventy years ago by Hans Bethe [1], it is an elegant though rather complicated approach that allows, in principle, to obtain all the eigenenergies and eigenstates for a certain class of microscopic one-dimensional Hamiltonians.

The most difficult problem of Bethe ansatz is complexity of the eigenfunctions. This often makes it very difficult to calculate the correlation functions.

Unless the excitation spectrum is gapless and linear in momentum (here the alternative methods of bosonization and conformal field theory can be used), the problem may become quite severe and was partially resolved only for models with Lorentz symmetry and for $T = 0$. In that case one can employ the formfactor expansion first suggested by Karowski *et. al* and then perfected by Smirnov. At nonzero temperature this expansion has problems related to singularities in the operator matrix elements (formfactors). Such singularities may exist even for models of non-interacting particles such as Quantum Ising model, provided the operators in question are nonlocal with respect to particle creation and annihilation operators.

In the second chapter of this thesis we explore this problem for the one-dimensional quantum Ising model (Ising model in a transverse magnetic field). This model consists in a chain of $S = 1/2$ spins with a nearest neighbor exchange interaction of their z -components and with a magnetic field applied in the x direction. This model can be recast as a model of free fermions at the expense of producing a highly nonlocal relationship between S^z operators and the fermion creation and annihilation operators. This nonlocality leads to singularities in the matrix elements of S^z . As far as the formfactor approach is concerned, the calculation of $S^z - S^z$ correlation function at $T \neq 0$ is as complicated problem as for other integrable models.

Fortunately the $S^z - S^z$ correlation function for the quantum Ising model admits an alternative representation [4], [5] and [6], which allows to circumvent the problems emerging in the formfactor expansion. This will allow us to derive long time asymptotics for the dynamical correlation function for the Ising model. These results give an idea of the kind of problems one should

expect to resolve to obtain similar expressions for correlation functions in other integrable models.

We start in section 2.1 by introducing the Ising model and its basic properties in some detail. Later, in section 2.2 we show how to calculate finite temperature correlators in the low energy regime where Lorentz symmetry emerges and a continuum description is appropriate. The results are written in terms of an expansion in powers of soliton density (virial expansion). Finally, in 2.3 we derive results for the dynamical correlator for the lattice high temperature regime where universality is lost ($T \gg J$).

In Chapter 3 we deal with a different kind of one dimensional system: the problem of two spin-1/2 Heisenberg chains interacting at a single point. To obtain the results we make extensive use of the method developed in [47] to transform the problem of two interacting Heisenberg chains into the problem of four independent one dimensional quantum Ising models. We find that since the operator describing the interaction is exactly marginal, correlations of physical operators have non-universal exponents.

1.2 Two-dimensional Systems

Two-dimensional physics is as full of marvels as one-dimensional ones. Its study has proven to be incredibly fruitful and has led to important discoveries in the past. For example, in 1980 the integral quantum Hall effect (QHE) [7] was discovered in two-dimensional electron systems followed by the discovery of the fractional QHE only two years later [8]. Both of these achievements were possible due to the realization of effectively 2D electron systems by con-

fining charge carriers into thin potential wells (MOSFET, GaAs heterostructures). Another remarkable discovery occurred in 1986 when high-temperature superconductivity was first observed in layered cuprates [11]. It is now widely agreed that their behavior is determined by physics of electrons and spins in two-dimensional copper-oxygen planes.

Not surprisingly then, the experimental realization of a two-dimensional layer of graphite (graphene) [12], [13] sparked an enormous amount of interest in this material. This one atom thick crystal provides a kind of two-dimensional electron system that is conceptually different from that mentioned in the previous paragraph. The realization of such a material was quite surprising because it was previously thought that such strictly two dimensional structure should not exist because it would be unstable due to divergent thermal fluctuations [10], [9].

One of the most remarkable properties of graphene is that its low energy excitations are well described by the spectrum of relativistic Dirac fermions. Interestingly then, we have a situation where quantum relativistic phenomena can be “tested” in a condensed matter experiment. From a more practical point of view, this material is very promising for applications in microelectronics and it may be a candidate to replace Si in the future. We have to wait to see if such important applications become a reality, but for the time being we have enough motivation to study graphene from the scientific point of view.

In Chapter 4 we explore the possibility of spin density wave formation in graphene that may be facilitated by the application of a magnetic field in the direction of the graphene plane. We argue that since the field splits the bands

creating a finite density of states at the Fermi surface, this situation is ideal for excitonic condensation of particle hole pairs. The most general form of the order parameter is presented and the critical temperature at which it will form is estimated. Critical fluctuations become extremely important in two dimensions so we pay special attention to them.

For completeness several appendices have been included. They contain details of important calculations and complementary background material we considered useful for the reader unfamiliar with some of the subjects treated.

Chapter 2

Order Parameter Correlators of the Quantum Ising Model

In this chapter we present some results obtained for the dynamical correlator of the order parameter field of the quantum Ising (QI) model. Although this model has been extensively studied we found room for our contribution.

For the sake of completeness and to aid the reader not familiar with the subject, in section 2.1 some basic facts about the Ising model are introduced. For a more complete review of important results regarding the Ising model the reader should consult references [14], [15] and [16]. In section 2.2 a virial expansion for the two-point correlation function is derived. Finally, in section 2.3, we obtain the dynamical correlator in the (lattice) high temperature limit.

2.1 Basics of the Ising Model

The Ising model (IM) was introduced in 1925 [17] as a simple theory of ferromagnetism and it remains until today, one of the most important models in statistical physics. It is the most elementary model of magnetic degrees of freedom with short range interactions and it possesses a wealth of interesting physical properties, for example, it undergoes a second order phase transition between a disordered and an ordered state. From the theoretical point of view, it also has the virtue that exact calculations can be performed. Physical realizations of the Ising model can be found in materials such as the dipolar-coupled ferromagnet $LiHoF_4$ [18].

We will start by describing the one dimensional Quantum Ising (QI) model [20] and later will discuss a useful correspondence between this model and the classical two-dimensional Ising model.

The QI model Hamiltonian is

$$H = -J \sum_n \left(\sigma_n^z \sigma_{n+1}^z + \frac{1}{\lambda} \sigma_n^x \right) \quad (2.1)$$

where σ^z, σ^x are the Pauli matrices, J is the nearest neighbor exchange interaction and J/λ is a transverse magnetic field. Now we can use the Jordan-Wigner transformation [19] to transform spins into fermionic degrees of freedom:

$$\sigma_n^z = - \prod_{m < n} (1 - 2c_m^\dagger c_m) (c_n^\dagger + c_n) \quad (2.2)$$

$$\sigma_n^x = 1 - 2c_n^\dagger c_n$$

Using this equivalence the Hamiltonian can be transformed into

$$H = -J \sum_n \left(c_{n+1}^\dagger c_n + c_n^\dagger c_{n+1} + c_n^\dagger c_{n+1}^\dagger + c_{n+1} c_n + \frac{1}{\lambda} (1 - 2c_n^\dagger c_n) \right) \quad (2.3)$$

Now, the usual Fourier mode transformation

$$c_n = \frac{1}{\sqrt{N}} \sum_p c_p e^{ipx_n} \quad (2.4)$$

can be used to simplify the Hamiltonian further

$$H = -J \sum_p \left(\frac{2}{\lambda} (\cos p - 1) c_p^\dagger c_p + i \sin p (c_{-p}^\dagger c_p^\dagger + c_{-p} c_p) + \frac{1}{\lambda} \right) \quad (2.5)$$

Finally using the Bogoliubov transformation the Ising chain is mapped into a system of non-interacting fermions:

$$H = \sum_p \epsilon(p) (F_p^\dagger F_p - 1/2) \quad (2.6)$$

where the single particle energy is given by,

$$\epsilon(p) = \frac{2J}{\lambda} \sqrt{(\lambda - 1)^2 + 4\lambda \sin^2(pa/2)} \quad (2.7)$$

with a being the lattice spacing and

$$F_p = u_p c_p - i v_p c_{-p}^\dagger \quad (2.8)$$

where

$$u_p = \cos \theta_p, \quad v_p = \sin \theta_p; \quad \tan 2\theta_p = \frac{\lambda \sin p}{\lambda \cos p - 1} \quad (2.9)$$

Hamiltonian (2.1) possesses a property of self-duality: the transformation $\mu_{n+1/2}^z = \prod_{j<n} \sigma_j^x$, $\mu_{n+1/2}^x = \sigma_n^z \sigma_{n+1}^z$ preserves both the commutation relations and the form of the Hamiltonian:

$$H = -J \sum_n \left(\frac{1}{\lambda} \mu_{n-1/2}^z \mu_{n+1/2}^z + \mu_{n+1/2}^x \right) \quad (2.10)$$

As follows from the form of the dispersion law (2.6), $\lambda = 1$ is the critical point, *i.e.* the point where the spectrum of excitations becomes gapless. It is easy to see that at $T = 0$ it separates the regions where $\langle \sigma^z \rangle \neq 0$ ($\lambda > 1$) and $\langle \mu_{n+1/2}^z \rangle \neq 0$ ($\lambda < 1$). Operators σ^z and μ^z are respectively called order and disorder parameter operators. The duality allows to study the correlation functions at one side of the transition only. For instance, a correlation function of σ^z at $\lambda > 1$ coincides with the correlation function for μ^z with $J, J/\lambda$ interchanged.

It is convenient to summarize some properties of the quantum Ising chain in a phase diagram (see Fig. 2.1). The diagram is divided in different regions, each one of them with different properties. In the *Quantum Paramagnetic* region the gap is larger than the temperature, the magnetic field is larger than the exchange of the order parameter and at $T = 0$ the system will be in a disordered ground state with $\langle \sigma^z \rangle = 0$. The *Quantum Critical* regime corresponds to T larger than the gap and the physics is dominated by the

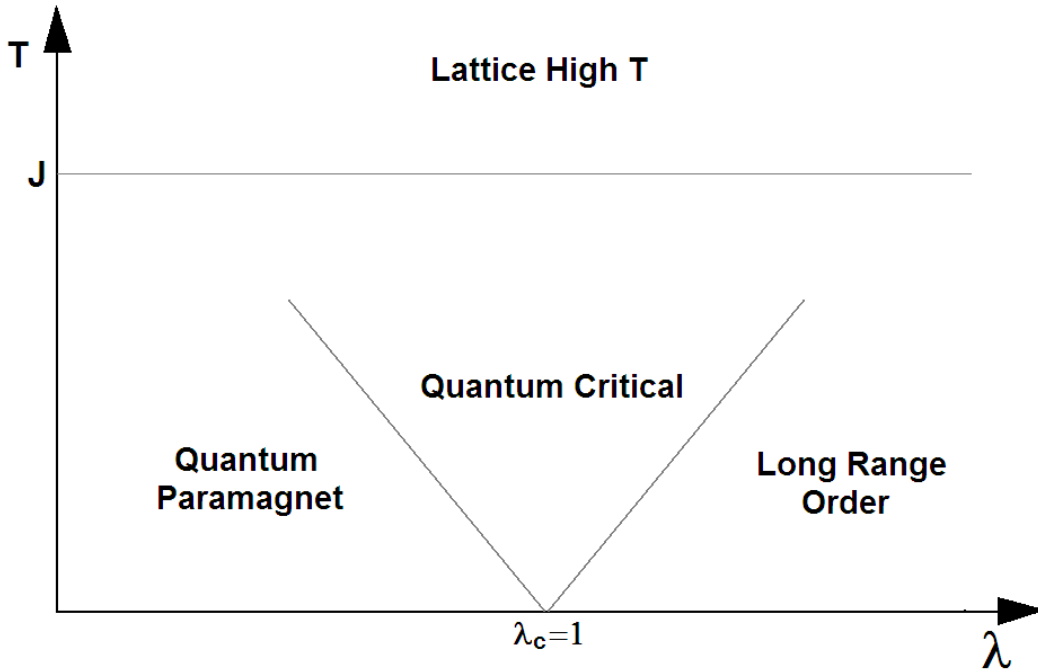


Figure 2.1: Phase diagram for the one dimensional quantum Ising model. There are three distinct low temperature regimes ($T \ll J$), in all of which Lorentz symmetry emerges and a field theory description is appropriate. In the *Lattice High T* ($T \gg J$) both Lorentz symmetry and universality are lost.

quantum critical point. In section 2.2 we will study primarily the *Long Range Order* region where the temperature is lower than the gap but now, since the magnetic field is smaller than the exchange of the order parameter, the correlation length diverges exponentially when $T \rightarrow 0$ and at $T = 0$ the system is in its ordered phase.

So far we have only mentioned regimes in which $T \ll J$. In these a continuum description is appropriate and one can take advantage of the emergent Lorentz symmetry. In section 2.3 we will study the situation when $T \gg J$ and universality is lost (*Lattice High T*).

Though one cannot observe a single fermion, the fermionic statistics can be indirectly tested by measuring the correlation functions of σ^x . The operator σ^x (as well as μ^x) is local in fermions:

$$\begin{aligned}\sigma^x(x) &= \sum_k e^{-iqx} \gamma(k) \gamma(k-q) \hat{F}_k \hat{F}_{q-k}, \quad \hat{F}_k = \hat{F}_{-k}^\dagger, \\ \gamma(k) &= \sqrt{1 + k/\epsilon(k)}.\end{aligned}\tag{2.11}$$

Its finite temperature correlation functions are just polarization loops; they clearly contain the Fermi distribution functions of the fermion fields F . Since the order (σ^z) and disorder parameter (μ^z) fields are nonlocal in terms of fermions, their correlation functions are more complicated.

2.1.1 Correspondence between 2D classical and 1D quantum Ising models

We now briefly explain the correspondence between the two dimensional (2D) classical Ising model and the quantum Ising chain. The energy of the 2D classical IM is,

$$E = - \sum_{r_x, r_y} [K_x \sigma(r_x, r_y) \sigma(r_x + 1, r_y) + K_y \sigma(r_x, r_y) \sigma(r_x, r_y + 1)] \tag{2.12}$$

The critical line in the anisotropic 2D Ising model is determined by the equation (see Fig. 2.2)

$$\sinh 2K_x \sinh 2K_y = 1 \tag{2.13}$$

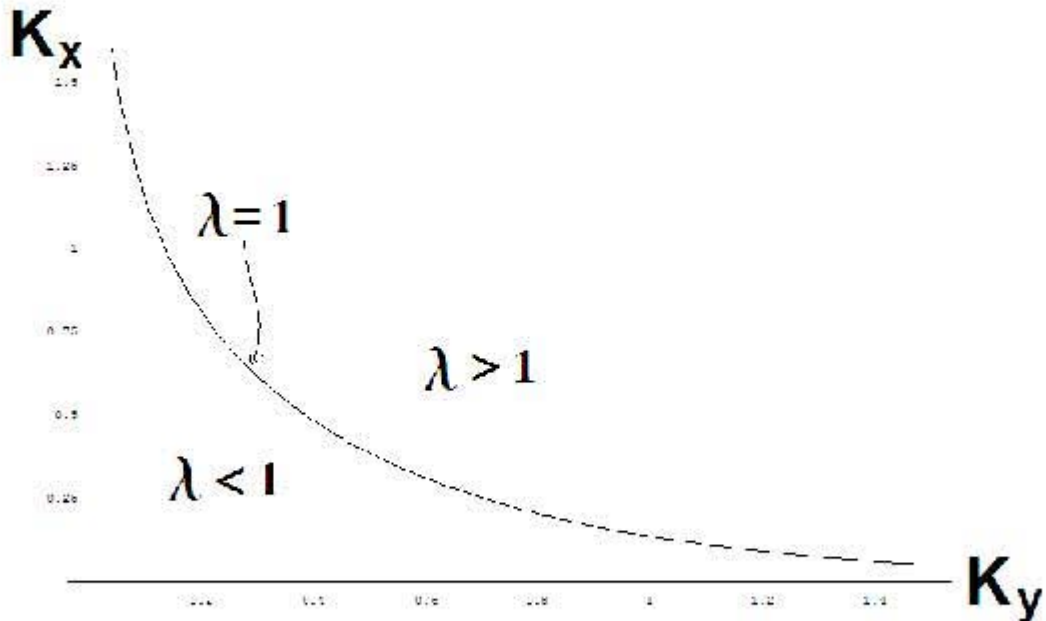


Figure 2.2: Critical line of the two dimensional classical Ising model. Above the line the system is in its ordered phase. When $\lambda < 1$ we are below the line and the system is in a paramagnetic state.

The couplings K are inversely proportional to temperature in the classical model. Large K 's correspond then to low temperature and we are in an ordered state above the critical line. Below the critical line, thermal fluctuations will disorder the system.

Let us choose the y direction as the (imaginary) time direction. Then one-dimensional QI model arises when the following continuum limit in the y direction ($K_y \rightarrow \infty$) is taken [21]:

$$\tau = r_y \tau_0, \quad r_y \rightarrow \infty, \quad \tau_0 = e^{-2K_y}$$

$$\sinh 2K_x \sinh 2K_y = \lambda \tag{2.14}$$

In this limit the classical model gives rise to the Hamiltonian of the one-dimensional quantum Ising model in a transverse magnetic field (2.1). More specifically, the correlators of the order parameter field in the classical model correspond to correlators of the quantum operator σ^z in the quantum one:

$$\langle \sigma(r_x, r_y) \sigma(0, 0) \rangle_C \rightarrow \langle \sigma^z(r_x, \tau) \sigma^z(0, 0) \rangle_Q \quad (2.15)$$

where τ is Matsubara time¹. Temperature and coupling in the quantum Ising model are related to the parameters of the classical model in the following way

$$\frac{J}{\lambda T} = M \tau_0 = M e^{-2K_y} \quad (2.16)$$

where M is the size of the classical system in the y (imaginary time) direction.

Furthermore, the phase transition mentioned before for the classical Ising model corresponds now to a quantum phase transition (QPT), that is, a transition at $T = 0$ for the quantum Ising chain. The role that thermal fluctuations played in the two dimensional classical system is now played by quantum fluctuations in the ground state of the quantum chain.

¹In the Matsubara time formalism it is exchanged by τ . Since we will make extensive use of this technique throughout this work a brief explanation of it is included in Appendix A.

2.2 Finite temperature correlation function: the virial expansion

In this section we rewrite the exact expression for the finite temperature two-point correlation function for the magnetization as a partition function of some field theory. This removes singularities and provides a convenient form to develop a virial expansion (the expansion in powers of soliton density).

2.2.1 Introduction

To calculate correlation functions in strongly correlated systems is not an easy task, even if the corresponding models happen to be integrable. For models with dynamically generated spectral gaps the most powerful technique is the formfactor approach pioneered by Karowski *et. al.* [22], [23] and perfected by Smirnov [24]. This approach works wonderfully for zero temperature, but encounters difficulties at $T \neq 0$ [25]. These difficulties are related to singularities in the operator matrix elements (formfactors). These singularities exist for operators nonlocal with respect to solitons, they originate from forward scattering processes and their treatment requires careful infrared regularization. Despite long efforts a correct regularization has not yet been found.

However, for models of free fermions (such as the XY model or the Quantum Ising model), there are alternative means to calculate the correlation functions which allow to bypass the above problems. These alternative approaches include the determinant representation of the correlation functions [26],[27] and the semiclassical method [28] (which may have much wider application,

see [29],[30]). For these results to have a greater use one has to establish their relationship with the formfactor approach. A step in this direction was made in [31] where the semiclassical results [28], [29],[30] were reproduced by summing up the leading singularities in the formfactor expansion. Such summation was restricted to the leading order in the soliton density $n \sim \exp(-M/T)$ (M is the spectral gap).

In what follows we describe a formfactor-based representation for correlation functions which, though in its present form is valid only for models of free fermions, is rather suggestive and may give rise to useful generalizations in the future. For the Quantum Ising (QI) model, which is the main object of this work, this procedure naturally gives rise to a virial expansion of the dynamical spin susceptibility.

In this section we will study the two-point correlation functions of the σ^z and μ^z operators in the “ordered” phase $\lambda > 1$. For technical reasons it will be convenient to work in the limit $|\lambda - 1| \ll 1$ when the spectral gap is much smaller than the bandwidth and one can formulate a continuous description. In this limit the excitation spectrum is relativistic

$$\epsilon(p) = \sqrt{M^2 + c^2 p^2} \tag{2.17}$$

where $M = 2J|\lambda - 1|$ and $c = 2Ja$. Energy and momentum of a quasi-particle are conveniently parameterized by a rapidity, θ , ($cp = M \sinh \theta$). Then the eigenstates of Hamiltonian (2.1) are labeled by sets of rapidities, $\{\theta_i\}$, such

that the energy and momentum of the system are equal to

$$E = M \sum_{i=1}^n \cosh \theta_i, \quad P = c^{-1} M \sum_{i=1}^n \sinh \theta_i. \quad (2.18)$$

Below we set $c = 1$.

2.2.2 Two-point Correlators

A convenient finite temperature expression for the two point correlation functions of σ^z and μ^z was derived by Bourgij and Lisovyy [4], [5]. This expression for the Matsubara time correlation function is manifestly free of singularities and has the following form:

$$\langle \sigma(\tau, x) \sigma(0, 0) \rangle = C M^{1/4} e^{-|x| \Delta(T)} \times \quad (2.19)$$

$$\sum_{N=0}^{\infty} \frac{T^{2N}}{(2N)!} \sum_{q_1, \dots, q_{2N}} \prod_{i=1}^{2N} \frac{e^{-|x| \epsilon_i - i \tau q_i - \eta(q_i)}}{\epsilon_i} \prod_{i>j} \left(\frac{q_i - q_j}{\epsilon_i + \epsilon_j} \right)^2$$

where τ is imaginary time. The same expression holds for μ^z , but with $2N$ replaced by $2N + 1$. $q = 2\pi T m$ (m integer), and $\epsilon(q) = \sqrt{M^2 + q^2}$. The terms in the exponents are ($\beta = 1/T$)

$$\eta(q) = \frac{2\epsilon(q)}{\pi} \int_0^{\infty} \frac{dx}{\epsilon^2(q) + x^2} \ln \coth[\beta \epsilon(x)/2], \quad (2.20)$$

and

$$\Delta(T) = \int_{-\infty}^{\infty} \frac{dp}{\pi} \ln \{ \coth[\beta \epsilon(p)/2] \} \quad (2.21)$$

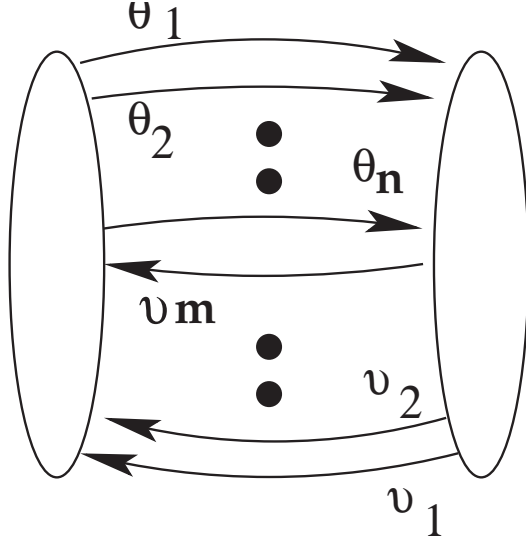


Figure 2.3: A graphic representation of Eq.(2.22). The ellipses are formfactors of σ operator. Lines with left arrows are $f^{(+)}(\theta) \exp[it\epsilon(\theta) + ixp(\theta)]$, lines with the right arrows are $f^{(-)}(\theta) \exp[-it\epsilon(\theta) - ixp(\theta)]$.

The symmetry breaking transition at $T = 0$ leads to a finite magnetization, $\langle \sigma \rangle = \pm [CM^{1/4}]^{1/2}$. This is reflected in the zeroth order term in Eq. (2.19).

In [31] Eq. (2.19) was rewritten in the form which allowed an analytic continuation for real time. The N -th term in the square brackets of Eq. (2.19) is given as ²

$$\sum_{n=1}^{2N} \frac{1}{n!(2N-n)!} \int \prod_{i=1}^n \frac{d\theta_i}{2\pi} f^{(+)}(\theta_i) e^{\tau\epsilon_i + ixp_i} \prod_{j=1}^{2N-n} \frac{d\theta'_j}{2\pi} f^{(-)}(\theta'_j) e^{-\tau\epsilon_j - ixp_j} \quad (2.22)$$

$$\times \frac{\prod_{i>k} \tanh^2[(\theta_i - \theta_k)/2] \prod_{j>p} \tanh^2[(\theta'_j - \theta'_p)/2]}{\prod_{i,p} \tanh^2[(\theta_i - \theta'_p + i0)/2]}$$

²In the paper [31] where this formula first appeared it was written in a simplified form valid in the limit $M \gg T$.

where,

$$f^{(+)}(\theta) = \frac{e^{\eta^{(+)}(\theta)}}{[e^{\beta\epsilon(\theta)} - 1]}, \quad f^{(-)}(\theta) = \frac{e^{-\eta^{(-)}(\theta)}}{[1 - e^{-\beta\epsilon(\theta)}]} \quad (2.23)$$

and

$$\eta^{(\pm)}(\theta) = \frac{iM \sinh \theta}{\pi} \int_{-\infty}^{\infty} \frac{dx \ln\{\coth[\beta\sqrt{M^2 + x^2}/2]\}}{x^2 - M^2 \sinh^2(\theta \pm i0)} \quad (2.24)$$

with $p(\theta) = M \sinh \theta$, $\epsilon(\theta) = M \cosh \theta$. As a check for consistency we can insert (2.22) into (2.19) and see that the dynamical correlator satisfies the periodic boundary condition

$$\langle \sigma(\tau + \beta, x) \sigma(0, 0) \rangle = \langle \sigma(\tau, x) \sigma(0, 0) \rangle \quad (2.25)$$

In (2.23) we have what seems to be bosonic distribution functions, in apparent contradiction with the fact that the excitations of the QI model are fermions. A more detailed analysis will reveal that there is no such contradiction. It can easily be shown that

$$\begin{aligned} \eta^{(\pm)}(\theta) &= \frac{i \sinh \theta}{\pi} PV \int_{-\infty}^{\infty} \frac{dx \ln\{\coth[\beta M \sqrt{1 + x^2}/2]\}}{x^2 - \sinh^2 \theta} \\ &\mp \ln\{\coth[\beta M \cosh \theta/2]\} \\ &\equiv i\eta(\theta) \mp \ln\{\coth[\beta M \cosh \theta/2]\} \end{aligned} \quad (2.26)$$

where we have defined η . Now we can rewrite

$$f^{(\pm)}(\theta) = e^{\beta\epsilon(\theta)/2 \pm (i\eta(\theta) - \beta\epsilon(\theta)/2)} f(\theta), \quad f(\theta) \equiv \frac{1}{e^{\beta\epsilon(\theta)} + 1} \quad (2.27)$$

where $f(\theta)$ is the Fermi distribution function.

In Eq.(2.22), n and $N - n$ are numbers of particles and antiparticles. Now we rearrange the double sum (2.22) in such a way that we first sum all terms which contain a fixed difference between numbers of particles and antiparticles $2N - 2n = 2k$. Then such term in Eq.(2.22) can be represented as an integral of the correlation function of a Gaussian field theory:

$$\frac{a_0^{-4k^2}}{(N-k)!(N+k)!} \int \prod_{i=1}^{N-k} \frac{d\theta_i}{2\pi a_0} f^{(+)}(\theta_i) e^{\tau\epsilon_i + \mathbf{i}xp_i} \times \quad (2.28)$$

$$\prod_{j=1}^{N+k} \frac{d\theta'_j}{2\pi a_0} f^{(-)}(\theta'_j) e^{-\tau\epsilon_j - \mathbf{i}xp_j} \langle \prod_i^{N-k} e^{\mathbf{i}\Phi(\theta_i + \mathbf{i}a)} \prod_j^{N+k} e^{-\mathbf{i}\Phi(\theta'_j - \mathbf{i}a)} e^{2k\mathbf{i}\Phi(\infty)} \rangle_0$$

where

$$\langle \Phi(\theta_1)\Phi(\theta_2) \rangle \equiv G_0(\theta_{12}) = -\ln \left[\frac{\tanh^2(\theta_{12}) + a_0^2}{R^2} \right] \quad (2.29)$$

and $a \gg a_0 \rightarrow 0$, $R \rightarrow \infty$. Here we have made use of the well known identity for the correlation function of exponents

$$\begin{aligned} \langle e^{\mathbf{i}\beta_1\Phi(\theta_1)} \dots e^{\mathbf{i}\beta_N\Phi(\theta_N)} \rangle &= e^{-\mathbf{i}\beta_i\beta_j G(\theta_i, \theta_j) - \frac{1}{2} \sum_i \beta_i^2 G(\theta_i, \theta_i)} \\ &= \prod_{i < j} \left(\frac{\tanh^2 \theta_{ij}}{a_0^2} \right)^{\beta_i \beta_j} \left(\frac{R}{a_0} \right)^{-(\sum_i \beta_i)^2} \end{aligned} \quad (2.30)$$

The correlator is different from zero only when

$$\sum_i \beta_i = 0. \quad (2.31)$$

Eq.(2.28) represents then one term in the perturbative expansion of the

partition function of the theory with the action

$$S = \frac{1}{2} \int d\theta_1 d\theta_2 \Phi(\theta_1) G_0^{-1}(\theta_{12}) \Phi(\theta_2) + \int \frac{d\theta}{2\pi a_0} V[\theta, \Phi(\theta)] \quad (2.32)$$

where

$$V = f^{(+)}(\theta) e^{\tau M \cosh \theta + i x M \sinh \theta} e^{i\Phi(\theta + ia)} \quad (2.33)$$

$$+ f^{(-)}(\theta) e^{-\tau M \cosh \theta - i x M \sinh \theta} e^{-i\Phi(\theta - ia)}$$

In this theory x , τ are external parameters. The field Φ lives on an infinite line in θ space. It is easy to see that the entire correlation function can be written as

$$\langle \sigma(\tau, x) \sigma(0, 0) \rangle = C M^{1/4} e^{-|x|\Delta(T)} Z_0(x, \tau) \lim_{R \rightarrow \infty} \sum_{k=-\infty}^{\infty} \frac{\langle e^{2ik\Phi(R)} \rangle_V}{a_0^{4k^2}} \quad (2.34)$$

where

$$Z_0 = \frac{\int D\Phi e^{-S[\Phi]}}{\int D\Phi e^{-S_0[\Phi]}} \quad (2.35)$$

and $\langle \dots \rangle_V$ stands for averaging with action (2.32). There is yet another way to write the correlator that is worth mentioning. We can insert (2.28) into (2.22) and easily see that we can rewrite

$$\langle \sigma(\tau, x) \sigma(0, 0) \rangle = C M^{1/4} e^{-|x|\Delta(T)} \sum_{N=0}^{\infty} \sum_{k=-N}^N \frac{\langle \alpha_+^{N-k} \alpha_-^{N+k} \rangle_0}{(N-k)!(N+k)!}$$

$$= C M^{1/4} e^{-|x|\Delta(T)} \langle \cosh(\alpha_+ + \alpha_-) \rangle_0 \quad (2.36)$$

where

$$\alpha_{\pm} = \int d\theta f^{(\pm)}(\theta) e^{\pm(\tau\epsilon(\theta) + \mathbf{i}xp(\theta))} e^{\pm\mathbf{i}\Phi(\theta \pm \mathbf{i}a)} e^{\mp\mathbf{i}\Phi(\infty)} \quad (2.37)$$

depend on x and τ .

Let us now go back to (2.34) and notice that this form leads to significant simplifications. The partition function can be written as an exponent of the free energy $Z_0 = \exp[-F(x, \tau)]$. The latter one is represented as a sum of the cumulants:

$$F = - \sum_{N=1}^{\infty} \frac{1}{(N!)^2} \int \prod_{i=1}^N \frac{d\theta_i}{2\pi a_0} f^{(+)}(\theta_i) e^{\tau\epsilon_i + \mathbf{i}xp_i} \times \quad (2.38)$$

$$\prod_{j=1}^N \frac{d\theta'_j}{2\pi a_0} f^{(-)}(\theta'_j) e^{-\tau\epsilon_j - \mathbf{i}xp_j} \langle \langle \prod_i e^{\mathbf{i}\Phi(\theta_i + \mathbf{i}a)} \prod_j e^{-\mathbf{i}\Phi(\theta'_j - \mathbf{i}a)} \rangle \rangle_0$$

where the subscript 0 stands for averaging with $V = 0$ and

$$Z_0(x, \tau) \langle e^{2\mathbf{i}k\Phi(R)} \rangle_V = \sum_{N=|k|}^{\infty} \frac{1}{(N-k)!(N+k)!} \int \prod_{i=1}^{N+k} \frac{d\theta_i}{2\pi a_0} f^{(+)}(\theta_i) e^{\tau\epsilon_i + \mathbf{i}xp_i} \times \quad (2.39)$$

$$\prod_{j=1}^{N-k} \frac{d\theta'_j}{2\pi a_0} f^{(-)}(\theta'_j) e^{-\tau\epsilon_j - \mathbf{i}xp_j} \langle \prod_i e^{\mathbf{i}\Phi(\theta_i + \mathbf{i}a)} \prod_j e^{-\mathbf{i}\Phi(\theta'_j - \mathbf{i}a)} e^{2\mathbf{i}k\Phi(R)} \rangle_0$$

2.2.3 Results and Conclusions

All transformations so far have been exact. Now we would like to concentrate on the causal Green's functions. To obtain them one has to replace τ with it in (2.22). Assuming that $T \ll M$, we consider the region of frequencies $|\omega| < 2M$, where the only terms of the expansion (2.22) contributing to the spectral

function are those which contain *equal* number of particles and antiparticles. As we shall demonstrate, all formfactor singularities are contained in the first term of expansion (2.38). Since $|f^{(+)}| \sim \exp(-\beta M) \ll 1$, $|f^{(-)}| \sim 1$, this expansion is in powers of soliton density $\exp(-\beta M)$. The first term is given by

$$\begin{aligned}
& -F^{(1)}(t, x) \\
&= \frac{1}{4\pi^2} \int d\theta_1 d\theta_2 f^{(+)}(\theta_1) f^{(-)}(\theta_2) \frac{\exp(i\{t[\epsilon(\theta_1) - \epsilon(\theta_2)] + x[p(\theta_1) - p(\theta_2)]\})}{\tanh^2(\theta_{12} + i0)/2} \\
&\approx \frac{1}{2\pi^2} \int d\theta dv f^{(+)}(\theta + v) f^{(-)}(\theta - v) \frac{\exp[ivM(t \sinh \theta + x \cosh \theta)]}{(v + i0)^2} \quad (2.40) \\
&\approx \theta(t - |x|) \left\{ \frac{1}{\pi} \int_{\tanh \theta < -|x|/t} d\theta f^{(+)}(\theta) f^{(-)}(\theta) M [(t \sinh \theta + x \cosh \theta)] \right. \\
&\quad \left. + \frac{2i}{\pi} g[\theta = \tanh^{-1}(x/t)] \right\}
\end{aligned}$$

where $g(\theta) = f^{(+)}(\theta) - f^{(-)}(\theta)$ and, as follows from (2.27)

$$f^{(+)}(\theta) f^{(-)}(\theta) = \frac{1}{4 \cosh^2[\beta\epsilon(\theta)/2]}. \quad (2.41)$$

In 2.40 we assumed that Mt , $(Tt)^{1/2} \gg [1 - (x/t)^2]^{-1/2}$. The higher order cumulants contain higher powers of $\exp(-\beta M)$ and also do not contain positive powers of t . This justifies keeping the exact distribution function in the real part of (2.40). This cannot be done for the imaginary part, since the second cumulant gives a time independent contribution $\sim \exp(-2\beta M)$. Within these limits we obtain the following results:

$$\langle \sigma(x, t) \sigma(0, 0) \rangle_T = CM^{1/4} \theta(t) e^{-\delta\Delta|x|} \exp \left\{ -\frac{1}{4\pi} \int dp \frac{|tv(p) - x|}{\cosh^2[\beta\epsilon(p)/2]} \right\}$$

$$-\frac{4i}{\pi} \exp[-\beta M / \sqrt{1 - (x/t)^2}] \Big\}, t > |x| \quad (2.42)$$

$$\langle \sigma(x, t) \sigma(0, 0) \rangle_T = C M^{1/4} \theta(t) \exp(-\Delta |x|), \quad |x| > t \quad (2.43)$$

$$\langle \mu(x, t) \mu(0, 0) \rangle_T = \langle \mu(x, t) \mu(0, 0) \rangle_{T=0} \langle \sigma(x, t) \sigma(0, 0) \rangle_T \quad (2.44)$$

where

$$\begin{aligned} \delta\Delta &= \frac{1}{\pi} \int dp \left[\ln \coth(\beta\epsilon/2) - \frac{1}{2 \cosh^2(\beta\epsilon/2)} \right] \\ &\sim \exp(-3\beta M) \end{aligned} \quad (2.45)$$

The imaginary part of (2.43) in the time-like domain $t > |x|$ reflects a quantum nature of the excitations. For $T = 0$ such imaginary part was first found in [33]. In the leading order in $\exp(-\beta M)$ Eq.(2.44) coincides with the one found in [28]. At $x = 0$ we have

$$\langle \sigma(x = 0, t > 0) \sigma(0, 0) \rangle \approx C M^{1/4} \exp \left[-t/\tau_0 + \frac{4i}{\pi} e^{-\beta M} + O(e^{-2\beta M}) \right]$$

where

$$\tau_0^{-1} = \frac{2T}{\pi} \frac{1}{e^{\beta M} + 1}. \quad (2.46)$$

Since single solitons are not directly observable, it is rather interesting to note that τ_0 contains the distribution function of a single soliton. It would be very interesting to see what happens in correlation functions in models containing

particles with fractional statistics.

Since our approach shares certain common features with the Fredholm determinant representation introduced by Korepin *et. al.* [26],[27], [34],[35], we feel obliged to comment on the subject. The main difference is that we do not represent the correlation functions as determinants though in certain limits this is possible. For instance, if one adopts the nonrelativistic limit $\theta \ll 1$ in action (2.32), it can be fermionized and rewritten as a theory of free fermions. Then by integrating over fermions one obtains the determinant representation. However, we would like to point out that such representation is not a goal in itself. By representing correlation functions as partition functions of some field theory one already achieves a lot since now one can concentrate on connected diagrams where it is easier to keep track of singularities. It is possible that acting along the lines of [37] one can obtain such representations for interacting models.

We also would like to warn against the direct comparison of Eq.(2.43) with a similar equation for the $\langle \sigma^- \sigma^+ \rangle$ correlation function in the XY model obtained in [26]. This warning is necessary because the XY model in magnetic field is rather similar to the QI model; the similarity increases when the magnetic field exceeds the band width so that the ground state becomes ferromagnetic. However, as was explained to us by Korepin (private communication), the formulae of [26] were obtained for the case of weak magnetic field the XY model spectrum is a gapless, which explains the difference in the final results.

2.3 High Temperature Limit of the Order Parameter Correlation Function

In this section we use the exact results for the anisotropic two-dimensional Ising model obtained by Bugrij and Lysovyy [6] to derive the expressions for dynamical correlation functions for the Quantum Ising model in one dimension at high temperatures.

2.3.1 Introduction

The previous attempts to calculate correlation functions of integrable models has mostly concentrated on the low energy (temperature) limit where field theory methods can be applied. In that case calculations are simplified due the emerging Lorentz symmetry and conformal symmetry (at criticality). Since such symmetries are absent for lattice theories at large temperatures, much less is known about the high temperature dynamics.

In this section we discuss the high temperature limit of the two-point correlation functions in the one-dimensional Quantum Ising (QI) model. Though this model has been extensively studied, the high temperature asymptotics are known only for the one site correlation function [38]. We extract these asymptotics from the general expressions for the correlation functions derived for the two-dimensional anisotropic classical Ising model (IM) in [6]. To translate them into quantum language, we will exploit the correspondence between a certain scaling limit of the two-dimensional classical IM and the one-dimensional QI model that was explained in full detail in section 2.1.

2.3.2 Quantum limit of the correlation functions

It was shown in [6] that the 2D anisotropic Ising correlator in the ferromagnetic phase ($\lambda > 1$) for the model of infinite size in the x direction and length N in the y -direction, can be written in the following form:

$$\langle \sigma(\tau, r_x) \sigma(0, 0) \rangle = \xi \xi_T e^{-|r_x| \Lambda^{-1}} \sum_{l=0}^{N/2} g_{2l}(r_x, \tau) \quad (2.47)$$

where,

$$g_n = \frac{e^{-n\Lambda^{-1}}}{n! N^n} \left[\frac{t_y(1-t_x^2)}{t_x(1-t_y^2)} \right]^{\frac{n^2}{2}} \sum_{\bar{q}} \prod_{j=1}^n \frac{e^{-|r_x| \gamma(\bar{q}_j) + i\tau \bar{q}_j - \eta(\bar{q}_j)}}{\sinh \gamma(\bar{q}_j)} F_n^2[\bar{q}] \quad (2.48)$$

$$F_n^2[\bar{q}] = \prod_{i < j}^n \frac{\sin^2((\bar{q}_i \tau_0 - \bar{q}_j \tau_0)/2)}{\sinh^2((\gamma_i + \gamma_j)/2)} = \left[\frac{\tau_0}{2} \right]^{n^2 - n} \prod_{i < j}^n \frac{(\bar{q}_i - \bar{q}_j)^2}{\sinh^2((\gamma_i + \gamma_j)/2)} \quad (2.49)$$

and,

$$\begin{aligned} \xi &= |1 - \lambda^{-2}|^{1/2} \\ \bar{q} \tau_0 &= q \\ \bar{q} &= 2\pi T m \quad (T^{-1} = \beta = N\tau_0) \end{aligned} \quad (2.50)$$

It is convenient to take the continuum limit as early as possible in the calculation, so we write the following,

$$\frac{t_y(1-t_x^2)}{t_x(1-t_y^2)} = \frac{\sinh 2K_y}{\sinh 2K_x} \rightarrow \frac{1}{4\lambda\tau_0^2} \quad (2.51)$$

$$\begin{aligned}
\cosh \gamma(q) &= \frac{\cosh 2K_y \cosh 2K_x - \sinh 2K_y}{\sinh 2K_x} + 2 \sin^2(q/2) \frac{\sinh 2K_y}{\sinh 2K_x} \\
&\rightarrow \frac{\bar{q}^2}{8\lambda} + \frac{1}{2}(\lambda^{-1} + \lambda)
\end{aligned} \tag{2.52}$$

$$\begin{aligned}
\cosh \bar{\gamma}(q) &= \frac{\cosh 2K_x \cosh 2K_y - \sinh 2K_x}{\sinh 2K_y} + 2 \sin^2(q/2) \frac{\sinh 2K_x}{\sinh 2K_y} \tag{2.53} \\
&\rightarrow 1 + 2(1 + \lambda^2) \left(1 - \frac{2\lambda}{1 + \lambda^2} \cos(q)\right) \tau_0^2 + \dots \\
&= 1 + \frac{\bar{\gamma}(q)^2}{2} + \dots
\end{aligned}$$

then,

$$\frac{N\bar{\gamma}(q)}{2} \rightarrow \frac{\sqrt{1 + \lambda^2}}{T} \left(1 - \frac{2\lambda}{1 + \lambda^2} \cos(q)\right)^{1/2} \tag{2.54}$$

where the arrows indicate that the continuum limit has been taken.

In other notations,

$$\begin{aligned}
\sinh(\gamma/2) &= \sqrt{M^2 + \frac{\bar{q}^2}{16\lambda}}, \\
\cosh(\gamma/2) &= \sqrt{1 + M^2 + \frac{\bar{q}^2}{16\lambda}}, \\
M^2 &= \frac{1}{4}(\sqrt{\lambda} - 1/\sqrt{\lambda})^2
\end{aligned} \tag{2.55}$$

In the continuum (that is quantum) limit (2.48) becomes

$$g_n = \frac{T^n}{n!} \left[\frac{1}{16\lambda} \right]^{\frac{n^2}{2}} \sum_{\bar{q}} \prod_{j=1}^n \frac{e^{-|r_x|\gamma(\bar{q}_j) + i\tau\bar{q}_j - \alpha(\bar{q}_j)}}{\sinh(\gamma_j/2) \cosh(\gamma_j/2)} \prod_{i < j}^n \frac{(\bar{q}_i - \bar{q}_j)^2}{\sinh^2((\gamma_i + \gamma_j)/2)} \tag{2.56}$$

where we have defined,

$$\alpha(\bar{q}) \equiv \eta(\bar{q}) + \Lambda^{-1} \quad (2.57)$$

and according to [6],

$$\Lambda^{-1} = \frac{1}{\pi} \int_0^\pi dp \log \coth \frac{N\bar{\gamma}(p)}{2} \quad (2.58)$$

$$\eta(\bar{q}) = \frac{1}{\pi} \int_0^\pi dp \frac{\cos(p) - e^{-\gamma(\bar{q})}}{\cosh \gamma(\bar{q}) - \cos(p)} \log \coth \frac{N\bar{\gamma}(p)}{2} \quad (2.59)$$

It is easy to see now that from (2.58) and (2.59) one gets,

$$\alpha(\bar{q}) = \frac{1}{\pi} \int_0^\pi dp \frac{\sinh \gamma(\bar{q})}{\cosh \gamma(\bar{q}) - \cos(p)} \log \coth \frac{N\bar{\gamma}(p)}{2} \quad (2.60)$$

As we mentioned in the introduction, we are interested in the nonuniversal or lattice high temperature limit, $T \gg J$. Notice that we chose to work with a notation in which T and τ are dimensionless variables and are related to the dimensionful ones in the following way,

$$T \rightarrow \frac{\lambda T}{J}; \quad \tau \rightarrow \frac{\tau J}{\lambda} \quad (2.61)$$

so that the high temperature regime in terms of our dimensionless variable is, $T \gg \lambda$. We will restore J at the end of the calculation. In the high

temperature regime we can make certain approximations, namely:

$$\coth \frac{N\bar{\gamma}(p)}{2} \approx \frac{T}{\sqrt{1+\lambda^2}} \left(1 - \frac{2\lambda}{1+\lambda^2} \cos(p)\right)^{-1/2} \quad (2.62)$$

and

$$\alpha(\bar{q}) \approx \frac{\sinh \gamma(\bar{q})}{\pi} \left[\log \left(\frac{T}{\sqrt{1+\lambda^2}} \right) \int_0^\pi \frac{dp}{\cosh \gamma(\bar{q}) - \cos(p)} - \frac{1}{2} \int_0^\pi dp \frac{\log \left(1 - \frac{2\lambda}{1+\lambda^2} \cos(p) \right)}{\cosh \gamma(\bar{q}) - \cos(p)} \right] \quad (2.63)$$

Now, using the table integrals from [39],

$$\int_0^\pi \frac{dx}{c \pm \cos x} = \frac{\pi}{\sqrt{c^2 - 1}}; \quad c^2 > 1 \quad (2.64)$$

$$\int_0^\pi dx \frac{\log \left(1 - \frac{2a}{1+a^2} \cos x \right)}{\left(\frac{1+b^2}{2b} - \cos x \right)} = \frac{2b\pi}{1-b^2} \log \frac{(1-ab)^2}{1+a^2}; \quad a^2 \leq 1, b^2 < 1 \quad (2.65)$$

we obtain

$$\alpha(\bar{q}) \approx \log \frac{T}{\lambda} - \log \left(1 - \lambda^{-1} e^{-\gamma(\bar{q})} \right) \quad (2.66)$$

Substituting these results into (2.56) we obtain

$$g_n \approx \frac{\lambda^n}{n!} \left[\frac{1}{16\lambda} \right]^{\frac{n^2}{2}} \sum_{\bar{q}} \prod_{j=1}^n (1 - \lambda^{-1} e^{-\gamma_j}) \quad (2.67)$$

$$\times \frac{e^{-|r_x|\gamma_j + i\tau\bar{q}_j}}{\sinh(\gamma_j/2) \cosh(\gamma_j/2)} \prod_{i < j}^n \frac{(\bar{q}_i - \bar{q}_j)^2}{\sinh^2((\gamma_i + \gamma_j)/2)}$$

2.3.3 Real time asymptotics.

To study the real time properties of the correlation function we will need to transform this sum into a n -variable integral in the complex plane, as it was done in [31]. The details of this calculation are given in Appendix B. The final result is

$$\langle \sigma^z(r_x, t) \sigma^z(0, 0) \rangle \sim \theta(t) \left(\frac{\lambda}{T} \right)^{|r_x|} e^{-R(t, |r_x|, \lambda)} \quad (2.68)$$

where R is given by Eq.(B.18). It can also be expressed in terms of the dispersion of fermions (solitons) in the 1-D quantum Ising model

$$\epsilon(k, \lambda) = \frac{2J}{\lambda} (1 + \lambda^2 - 2\lambda \cos ka)^{1/2} \quad (2.69)$$

where a is the lattice spacing. Considering this and restoring dimensions according to (2.61), the result for $R(t, |r_x|, \lambda)$ can then be written as

$$\begin{aligned} R(t, |r_x|, \lambda) &= \frac{2}{\pi} \int_{-\pi/a}^{\pi/a} dk (v(k, \lambda)t - |r_x|a) \theta(v(k, \lambda)t - |r_x|a) \quad (2.70) \\ &= \frac{1}{\pi} \int_{-\pi/a}^{\pi/a} dk [|x - v(k, \lambda)t| - |x|] \end{aligned}$$

where $x = |r_x|a$, and,

$$v(k, \lambda) = \frac{\partial \epsilon(k, \lambda)}{\partial k} = \frac{Ja \sin ka}{\sqrt{\lambda}(M^2 + \sin^2(ka/2))^{1/2}} \quad (2.71)$$

It can be easily shown that,

$$\max [v(k, \lambda)] = \frac{2Ja}{\lambda} \quad (2.72)$$

for any value of λ . Because of the step function inside the integral in (2.70) this means that, $R(t, |r_x|, \lambda)$ vanishes at $t < \lambda|r_x|/2J$ and has the following form:

$$R(t, |r_x|, \lambda) = t f\left(\frac{t}{r_x}, \lambda\right) \theta\left(\frac{2Jt}{\lambda} - |r_x|\right) \quad (2.73)$$

Hence, there is no time dependence in the long distance correlator at $t < \lambda|r_x|/2J$. This is a direct consequence of causality: even excitations with the maximum velocity cannot travel the distance $|r_x|$ in such a short time.

An analytic expression can be obtained for R ,

$$R(t, |r_x|, \lambda) = \frac{2t}{\pi} \left[\epsilon(k_0^+, \lambda) - \epsilon(k_0^-, \lambda) - \frac{|r_x|a}{t} (k_0^+ - k_0^-) \right] \theta\left(\frac{2Jt}{\lambda} - |r_x|\right) \quad (2.74)$$

where,

$$\cos k_0^\pm a = \lambda \left(\frac{|r_x|}{2Jt}\right)^2 \mp \sqrt{\lambda^2 \left(\frac{|r_x|}{2Jt}\right)^4 - (1 + \lambda^2) \left(\frac{|r_x|}{2Jt}\right)^2 + 1} \quad (2.75)$$

with

$$0 < k_0 a < \pi$$

To give a more explicit expression for the correlation function (2.68), we

will calculate $R(t, |r_x|, \lambda)$ in two limits where the expression (2.74) considerably simplifies. For $\lambda \rightarrow 1$ we have

$$\langle \sigma^z(r_x, t) \sigma^z(0, 0) \rangle \sim \theta(t) \left(\frac{J}{T} \right)^{|r_x|} \exp \left\{ -\frac{4}{\pi} \left[\sqrt{(2Jt)^2 - |r_x|^2} - \left(\frac{\pi}{2} - \arcsin \frac{|r_x|}{2Jt} \right) |r_x| \right] \theta(2Jt - |r_x|) \right\} \quad (2.76)$$

At $\lambda \gg 1$ (strongly ferromagnetic limit) we obtain,

$$\langle \sigma^z(r_x, t) \sigma^z(0, 0) \rangle \sim \theta(t) \left(\frac{J}{T} \right)^{|r_x|} \exp \left\{ -\frac{4}{\pi} \left[\sqrt{\left(\frac{2Jt}{\lambda} \right)^2 - |r_x|^2} - \left(\frac{\pi}{2} - \arcsin \frac{|r_x| \lambda}{2Jt} \right) |r_x| \right] \theta \left(\frac{2Jt}{\lambda} - |r_x| \right) \right\} \quad (2.77)$$

Notice that the only difference in the time dependence in both regimes is that of a rescaling of time ($t \rightarrow t/\lambda$).

Remember now that all the results were obtained for the ferromagnetic phase ($\lambda > 1$). For the paramagnetic phase, equation (2.47) becomes a sum over g_{2l+1} . It turns out that this change has a little effect over the high temperature correlator. In fact, the form of R does not change and one can easily derive the following result for $\lambda < 1$,

$$\langle \sigma^z(r_x, t) \sigma^z(0, 0) \rangle \sim \theta(t) \left(\frac{J}{\lambda T} \right)^{|r_x|} e^{-R(t, |r_x|, \lambda)} ; \quad T \gg J/\lambda \quad (2.78)$$

The ‘‘high temperature regime’’ has to be redefined because in the paramagnetic phase the transverse field becomes larger than the spin-spin coupling.

2.3.4 Conclusions

Let us now discuss qualitative features of Eq.(2.68). As expected, at zero time we get the standard result for the one-dimensional classical Ising model:

$$\langle \sigma^z(r_x, 0) \sigma^z(0, 0) \rangle \sim \left(\frac{J}{T} \right)^{|r_x|} \quad (2.79)$$

At least in the framework of the adopted approximation $|r_x| \gg 1$, this result persists at nonzero time at times smaller than $\lambda|r_x|/2J$. Recall that J/λ is the coefficient in front of σ^x in the Hamiltonian. Without this term there is no dynamics. Hence the obtained time dependence is a quantum effect, as one expects.

If $2tJ \gg \lambda|r_x|$ one gets the following approximation:

$$\langle \sigma^z(r_x, t) \sigma^z(0, 0) \rangle \sim \theta(t) e^{-|r_x|(\log \frac{T}{J} - 2) - \frac{8Jt}{\pi\lambda} - \frac{\lambda|r_x|^2}{\pi Jt}} \quad (2.80)$$

This is different from the Gaussian in t behavior which holds for $T = \infty$ for $|r_x| = 0$ [38].

Chapter 3

Crossed Spin-1/2 Heisenberg Chains as a Quantum Impurity Problem

Using equivalencies between different models we reduce the model of two spin-1/2 Heisenberg chains crossed at one point to the model of free fermions. The spin-spin correlation function is calculated by summing the perturbation series in the interchain interaction. The result reveals a power law decay with a nonuniversal exponent.

3.1 Introduction

Presence of impurities in interacting systems causes nonlinear effects which may result in a nontrivial scaling of thermodynamic quantities and correlation functions. Examples of impurity models discussed in the literature include

various versions of the Kondo problem (a quantum spin in a noninteracting metallic host) and the Kane-Fisher or Boundary Sine-Gordon problem (a local static potential in a one-dimensional Luttinger liquid). They have numerous experimental applications in physics of diluted magnetic alloys ([40],[41]) and in such areas as interedge tunnelling in Quantum Hall effect (see, for example, [42],[43]). As a rule the impurity scattering in these models scales to strong coupling. The latter fixed point is rather simple in nature (fully screened spin in the Kondo problem, severed chain in the Kane-Fisher one). The exclusion is the fixed point in the underscreened Kondo problem where the fixed point occurs at an intermediate coupling first predicted in [44]. This fixed point is characterized by non-trivial universal indices.

In the present work we would like to call the attention to the situation when the operator describing a scattering on the impurity is exactly marginal (that is, its scaling dimension is equal to the dimension of space-time, which in the present case is 2). Since such interaction does not flow under renormalization, the results for the correlation functions are bound to depend on the bare coupling constant. In particular, such situation exists when the underlying impurity problem is equivalent to a problem of noninteracting fermions scattering on a scalar potential. An interesting situation emerges when the fermion operators and observables are mutually nonlocal. In that case calculation of correlation functions of the physical fields still constitutes a nontrivial problem resulting in nonuniversal scaling dimensions.

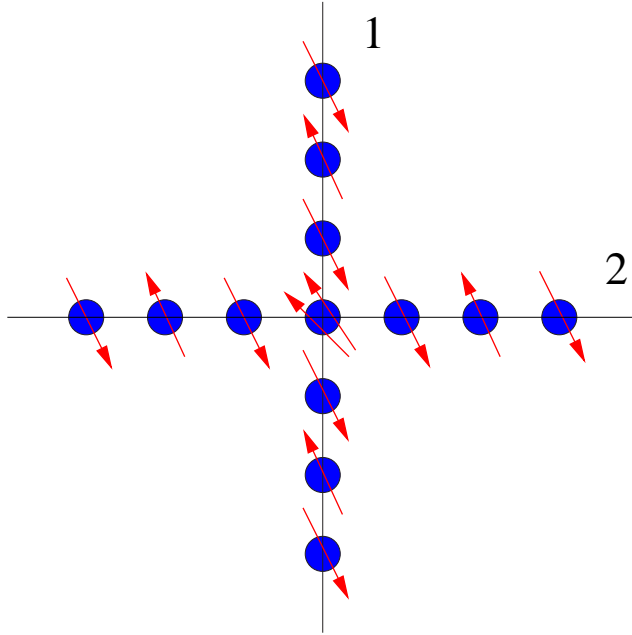


Figure 3.1: Pictorial depiction of Hamiltonian 3.1. Heisenberg chains consist of spins (arrows) located at each site that interact with its nearest neighbor via exchange interaction. Additionally, there is also interaction between chains at a single site located at $x = 0$.

3.2 The Model: two Heisenberg chains interacting at a single point

One experimentally relevant realization of the Marginal Quantum Impurity problem is provided by the model of two spin-1/2 Heisenberg chains interacting at a single point by the exchange interaction (see Fig. 3.1):

$$\begin{aligned}
 H = & \sum_{n=-\infty}^{+\infty} J[\mathbf{S}_1(n) \cdot \mathbf{S}_1(n+1) + \mathbf{S}_2(n) \cdot \mathbf{S}_2(n+1)] \\
 & + J_{\perp} \mathbf{S}_1(0) \cdot \mathbf{S}_2(0)
 \end{aligned} \tag{3.1}$$

where $|J_{\perp}| \ll J$. This model can be treated as a particular version of the spin ladder problem. To understand this model it is better to start with a single chain.

The spin-1/2 one dimensional Heisenberg model is very simple but it has many interesting (nontrivial) properties and it describes real physical systems. Realizations of such a model can be found in quasi one-dimensional materials where the exchange interaction in one direction is much larger than in the other two. Measurements made at an intermediate energy scale between the two exchange energies just mentioned will reveal one dimensional properties of the three dimensional solid. Furthermore, some of these materials have local magnetic moments with two low-lying levels so that an effective spin-1/2 model gives an appropriate description.

The one dimensional Heisenberg chain is exactly solvable via the Bethe-ansatz method [1] and one can thus in principle obtain its eigenfunctions and eigenenergies. It turns out though, that it is very hard to find correlation functions using this solution and it is much easier to use a different method. We use the Bosonization approach [45], [46] which gives a much simpler description of the low energy properties of the system. For a brief review of this approach see Appendix C.

The low energy sector of a single one dimensional antiferromagnetic spin-1/2 Heisenberg chain can then be described by the following Hamiltonian,

$$H = \frac{v_s}{2} \int dx [\Pi^2(x) + \partial_x \phi^2(x)] \quad (3.2)$$

where the velocity $v_s \sim Ja$, with a being the lattice spacing. Using the cor-

respondence between bosonic field operators and the spin operators of the original theory shown in Appendix C, the bosonic form of the interchain interaction term in (3.1) can be deduced.

One can transform the bosonic version of the Hamiltonian for the two interacting chains (3.1) further by employing the technique developed in [47] (see also Appendix D) and rewrite the Hamiltonian as the model of four pairs of massless real (Majorana) fermions coupled at point $x = 0$

$$H = \int dx \sum_{a=0}^3 \left[\frac{iv}{2} (-R_a \partial_x R_a + L_a \partial_x L_a) + ig_a \delta(x) (R_a L_a) \right] \quad (3.3)$$

where $g_i = J_{\perp} a_0$ ($i = 1, 2, 3$); $g_0 = -3g_1$ and $v = \pi J a_0 / 2$ is the spinon velocity. The fermion operators satisfy the standard anticommutation relations

$$\begin{aligned} \{R_a(x), R_b(y)\} &= \{L_a(x), L_b(y)\} = \delta_{ab} \delta(x - y) \\ \{R_a(x), L_b(y)\} &= 0 \end{aligned} \quad (3.4)$$

and are real, that is $R^+ = R, L^+ = L$. The ratio g_0/g_a can be changed by introduction of the four-spin interaction [48]. Thus the model of interacting spins is reduced to the model of non-interacting fermions. This representation respects the original symmetry of the problem: the fermions $a = 1, 2, 3$ transform as an SU(2) triplet and the 0-th fermion is an SU(2) singlet. Fermionization of one-dimensional spin models has a long history going back to the work by Jordan and Wigner [19]. It is well known that a single spin-1/2 Heisenberg chain can be represented as a model of fermions which interaction depends on the anisotropy (see Appendix C). At the isotropic point this interaction is

quite strong. Therefore it is interesting to note that though a single isotropic spin-1/2 Heisenberg chain cannot be described as a model of noninteracting fermions, the two chain model can. Naturally, the spin operators of the original Heisenberg chains are nonlocal with respect to the Majorana fermions (the relationship between them resembles the one given by the Jordan-Wigner transformation). For that reason the problem of correlation functions still remains nontrivial. To calculate the spin correlators we will employ an alternative representation of model (3.3), namely, in the form of four quantum Ising models:

$$H = \sum_{a=0}^3 H_{Is}^a, \quad H_{Is}^a = H_{crit}^a + g_a \epsilon_a(x=0) \quad (3.5)$$

where H_{crit} is the Hamiltonian of the critical Ising model and $\epsilon(x, \tau)$ is the energy density field. The quantum Ising model is described by the Hamiltonian

$$H = -J \sum_n (\sigma_n^z \sigma_{n+1}^z + h \sigma_n^x) \quad (3.6)$$

The Jordan-Wigner transformation brings it to the fermionic form. The order parameter field $\sigma(x)$ of the Ising model is the continuum limit of σ_n^z , the energy density field is the continuum limit of σ_n^x . At $h < 1$ field σ has a nonzero vacuum average $\langle \sigma \rangle \neq 0$. Hamiltonian (3.6) can be rewritten in the dual form

$$H = -J \sum_n (h \mu_{n-1/2}^z \mu_{n+1/2}^z + \mu_{n+1/2}^x) \quad (3.7)$$

where the operators

$$\mu_{n+1/2}^z = \prod_{j \leq n} \sigma_j^x, \quad \mu_{n+1/2}^x = \sigma_n^z \sigma_{n+1}^z \quad (3.8)$$

obey the same commutation relations as the Pauli matrices σ^z, σ^x . The so-called disorder parameter field $\mu(x)$ is defined as the continuum limit of the operator $\mu_{n+1/2}^z$. It is clear that $\langle \mu \rangle \neq 0$ at $h > 1$. At $h = 1$ the model (3.6) coincides with its dual (3.7). Since σ and μ cannot have nonzero ground state expectation values simultaneously, at $h = 1$ their averages vanish and the model is quantum critical. At this point the Majorana fermion becomes massless. Thus model (3.6) with $h = 1$ is equivalent to the model of one species of massless Majorana fermions.

The advantage of the Ising model representation is that the original spin fields of the Heisenberg models can be written as

$$\begin{aligned} \mathbf{S}_1(j) + \mathbf{S}_2(j) &= \frac{i}{2} \{[\mathbf{R} \times \mathbf{R}] + [\mathbf{L} \times \mathbf{L}]\} + (-1)^j \mathbf{n}_+(x) \\ \mathbf{S}_1(j) - \mathbf{S}_2(j) &= \frac{i}{2} \{R_0 \mathbf{R} + L_0 \mathbf{L}\} + (-1)^j \mathbf{n}_-(x) \end{aligned} \quad (3.9)$$

where the most relevant parts of the spin operators given by the staggered magnetizations \mathbf{n}_\pm are expressed as local combinations of the order and disorder parameters of the Ising models [47]:

$$n_+^x = \sigma_1 \mu_2 \sigma_3 \mu_0, \quad n_+^y = \mu_1 \sigma_2 \sigma_3 \mu_0, \quad n_+^z = \sigma_1 \sigma_2 \mu_3 \mu_0 \quad (3.10)$$

In the expression for \mathbf{n}_- one has to interchange σ and μ .

3.3 Correlators for Staggered Magnetization

Correlation functions of the Ising model fields and their properties are well known and we are going to use this knowledge to calculate the correlators of the perturbed model (3.3). Using Eqs.(3.10) it is easy to relate the desired spin correlators to the correlation functions of the perturbed Ising model:

$$\langle n_\alpha^a(\tau_1, x_1) n_\beta^a(\tau_2, x_2) \rangle = \quad (3.11)$$

$$\begin{aligned} & G_{\sigma, g_1}^2(\tau_{12}; x_1, x_2) G_{\mu, g_1}(\tau_{12}; x_1, x_2) G_{\mu, g_0}(\tau_{12}; x_1, x_2) \\ & + (2\delta_{\alpha\beta} - 1) G_{\mu, g_1}^2(\tau_{12}; x_1, x_2) G_{\sigma, g_1}(\tau_{12}; x_1, x_2) G_{\sigma, g_0}(\tau_{12}, x_1, x_2) \end{aligned}$$

where,

$$G_{\mu, g}(\tau; x_1, x_2) \equiv \langle \langle \mu(\tau, x_1) \mu(0, x_2) \rangle \rangle_g \quad (3.12)$$

$$G_{\sigma, g}(\tau; x_1, x_2) \equiv \langle \langle \sigma(\tau, x_1) \sigma(0, x_2) \rangle \rangle_g \quad (3.13)$$

and α, β label the chain to which the operator corresponds (1 or 2). Notice that the correlators remain translationally invariant only in time direction. To simplify the calculations we will consider the above correlation functions only at $x_{1,2} = 0$. To obtain these correlators we sum the leading logarithms in the perturbation expansion in small g_a .

Namely, the Ising order parameter field correlator, $\langle \langle \sigma(\tau_a) \sigma(\tau_b) \rangle \rangle$ (we omit the space coordinate x assuming $x = 0$) can be obtained by calculating the

following series,

$$\langle\langle\sigma(\tau_a)\sigma(\tau_b)\rangle\rangle_g = \sum_{n=0}^{+\infty} \frac{g^n}{n!} C_n \quad (3.14)$$

where,

$$C_n \equiv \int d\tau_1 \dots d\tau_n \langle\langle\sigma(\tau_a)\sigma(\tau_b)\varepsilon(\tau_1)\dots\varepsilon(\tau_n)\rangle\rangle_0 \quad (3.15)$$

and $\langle\langle\rangle\rangle_0$ denotes the irreducible correlator in the unperturbed system and,

$$\varepsilon \equiv iRL(x=0) \quad (3.16)$$

is the Ising model energy density at the impurity point.

Only the largest divergent terms will be kept at each order in g . The irreducible correlators under consideration will have its largest divergencies in the regions where each of the τ_i 's approach either τ_a or τ_b corresponding to the fusion of ε and σ operators. Divergencies corresponding to the fusion of ε operators are not present in the irreducible correlation functions being cancelled by the corresponding divergencies in the partition function. To calculate the leading logarithms we take advantage of the Operator Product Expansion (OPE) for the critical Ising model [49]:

$$\varepsilon(\tau_i)\sigma(\tau_{a,b}) = \frac{1}{2^{|\tau_{a,b} - \tau_i|}} \sigma(\tau_{a,b}) + \dots \quad (3.17)$$

where the dots stand for less relevant terms. The most divergent part of C_n is

given by

$$C_n \approx \left[2 \ln \left(\frac{|\tau_{ab}|}{\tau_0} \right) \right]^n \quad (3.18)$$

where τ_0 is an ultraviolet cutoff. The factor 2^n comes from the number of regions with divergent integrand that exist (that is to say, the number of ways the n different τ_i variables can approach either τ_a or τ_b) and the logarithm comes from integrating over this regions.

Now, replacing this result into (3.14) is easy to see that,

$$\begin{aligned} G_{\sigma,g} &= \langle \sigma(\tau_a) \sigma(\tau_b) \rangle_0 \left(\frac{\tau_0}{|\tau_{ab}|} \right)^{-2g} \\ &= \frac{1}{|\tau_{ab}|^{\frac{1}{4}}} \left(\frac{\tau_0}{|\tau_{ab}|} \right)^{-2g} \end{aligned} \quad (3.19)$$

where $\langle \sigma(\tau_a) \sigma(\tau_b) \rangle_0 \sim |\tau_{ab}|^{-1/4}$ is the correlator of the unperturbed system.

Similar considerations are valid for the perturbation series for the disorder parameter, $\langle \mu(\tau_a) \mu(\tau_b) \rangle$. The only difference is that the OPE contains minus sign [49]:

$$\varepsilon(\tau_i) \mu(\tau_{a,b}) = -\frac{1}{2|\tau_{a,b} - \tau_i|} \mu(\tau_{a,b}) + \dots \quad (3.20)$$

Then the same steps that lead to (3.19), now lead to:

$$\begin{aligned} G_{\mu,g} &= \langle \langle \mu(\tau_a) \mu(\tau_b) \rangle \rangle_0 \left(\frac{\tau_0}{|\tau_{ab}|} \right)^{2g} \\ &= \frac{1}{|\tau_{ab}|^{\frac{1}{4}}} \left(\frac{\tau_0}{|\tau_{ab}|} \right)^{2g} \end{aligned} \quad (3.21)$$

where $g = g_1$ for μ_a ($a=1,2,3$) operator and g_0 for the μ_0 operator.

Substituting (3.19,3.21) into (3.11) we obtain

$$\langle \mathbf{n}_\alpha(\tau_a) \cdot \mathbf{n}_\beta(\tau_b) \rangle = \frac{3}{|\tau_{ab}|} \left[\left(\frac{\tau_0}{|\tau_{ab}|} \right)^{-2\tilde{g}} + (2\delta_{\alpha\beta} - 1) \left(\frac{\tau_0}{|\tau_{ab}|} \right)^{2\tilde{g}} \right] \quad (3.22)$$

where $\tilde{g} = (g_1 - g_0)$. The nonuniversal power law behavior of the spin-spin correlation functions is reflected in the power law behavior of the local magnetic susceptibility:

$$\chi(x=0) \sim (T/T_0)^{2\tilde{g}} + (T/T_0)^{-2\tilde{g}}, \quad T_0 \sim J \quad (3.23)$$

As one may expect, the susceptibility does not depend on the sign of the interchain interaction. Since the perturbing impurity operator is exactly marginal, it does not generate any nontrivial corrections to the specific heat. The impurity magnetic susceptibility diverges with a nonuniversal index (3.23).

Thus we have found a nontrivial example of the impurity problem where strong correlations in the bulk generate nonuniversal scaling dimensions. This model may be a member of a class of models which can be formulated as a scattering problem for free particles, whose creation and annihilation operators and the observables are mutually nonlocal.

Chapter 4

Spin Density Wave Formation in Graphene Facilitated by in-plane Magnetic Field

We suggest that by applying a magnetic field lying in the plane of graphene layer one may facilitate an excitonic condensation of electron-hole pairs with opposite spins. The Spin Density Wave order parameter has $U(1) \times O(4)$ symmetry. Our calculations yield a conservative estimate for the Berezinskii-Kosterlitz-Thouless transition temperature $T_{BKT} \sim 10^{-2} - 10^{-1} B$. Below T_{BKT} the system is in insulating state with a finite spin conductivity and disordered spin fluctuations.

4.1 Introduction

Since its experimental realization three years ago [12], [13], graphene (graphite monolayer) has attracted an enormous amount of attention. From the theoretical point of view it has the unique and beautiful property that its quasiparticle spectrum can be described by massless Dirac spinors. From a more practical point of view, it holds the promise for future applications, particularly in microelectronics.

The present introduction is organized as follows. In 4.1.1 we present a brief summary of some basic facts about graphene that we considered essential to be able to understand the rest of the chapter. Later, in 4.1.2 we motivate our study of SDW formation facilitated by the application of a magnetic field in the direction of the plane of the graphene layer.

4.1.1 Basics of Graphene

Graphene is a material that consists of a single layer of graphite in which carbon atoms are arranged in a tightly packed honeycomb lattice configuration (see Fig. 4.1). Even though it was only recently realized experimentally, graphene has been studied theoretically for many years, not only because of its peculiar properties but also because 2D graphite layers are the basis of other structures such as buckyballs and carbon nanotubes.

The current literature about graphene is immense; as far as the band structure is concerned, the most elementary information can be found in [50]. The spectrum of the single layer graphene is well described by the tight-binding

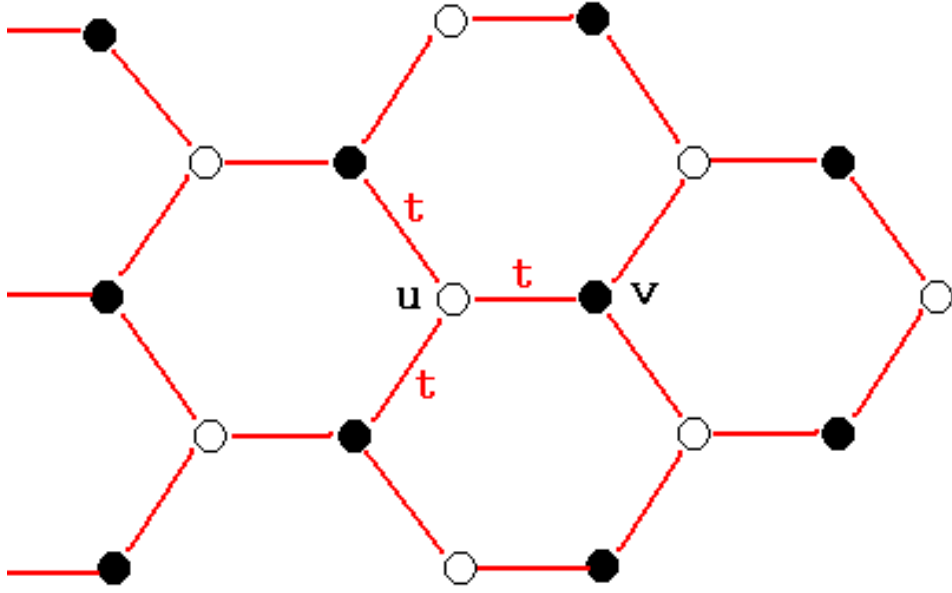


Figure 4.1: Graphene's hexagonal lattice. Carbon atoms are arranged into two overlapping triangular lattices (u and v). We consider nearest neighbor hopping amplitude t .

Hamiltonian with tunneling to nearest neighbors:

$$H_0 = -t \sum_{\mathbf{r}, i\sigma} u_{\sigma}^+(\mathbf{r}) v_{\sigma}(\mathbf{r} + \mathbf{b}_i) + h.c. \quad (4.1)$$

where \mathbf{r} belong to a triangular lattice (see Fig. 4.1). By introducing the Fourier transform of the creation operators in the usual way, this Hamiltonian can be easily diagonalized. As a result, the energy spectrum of quasiparticles is found to be

$$\epsilon(\mathbf{k}) = \pm t \sqrt{1 + 4 \cos(3k_x a/2) \cos(\sqrt{3}k_y a/2) + 4 \cos^2(\sqrt{3}k_y a/2)} \quad (4.2)$$

where t is the nearest neighbor hopping energy and a is the spacing between

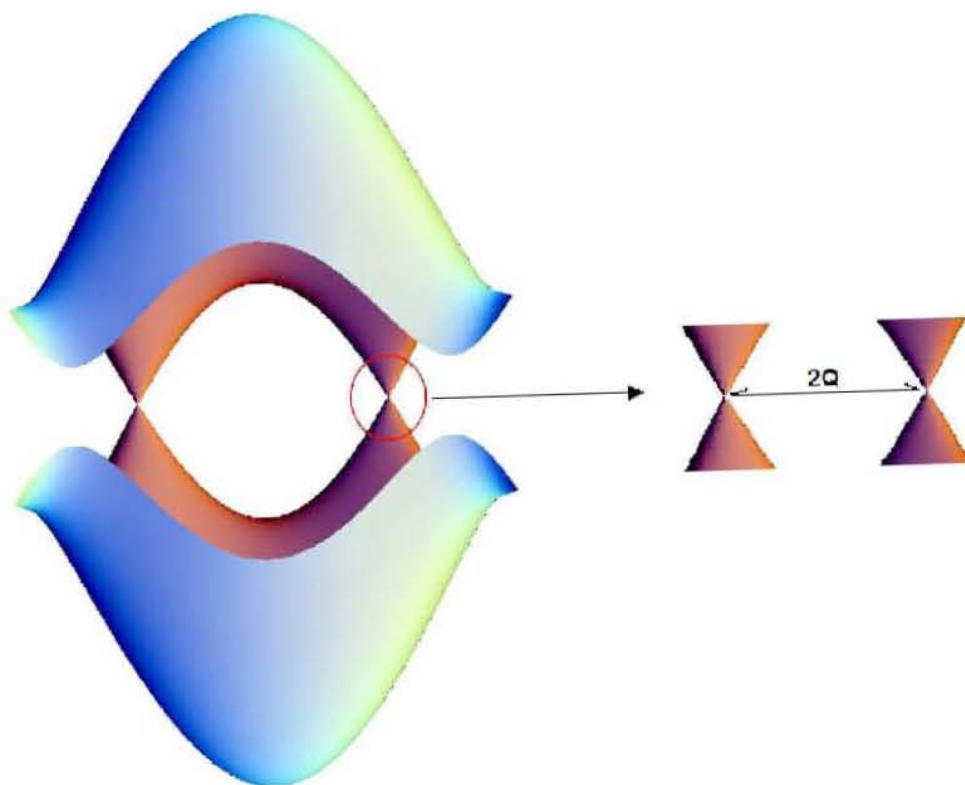


Figure 4.2: The spectrum of quasiparticles (4.2) as obtained from the nearest neighbor hopping Hamiltonian. Valence and conduction bands touch at two points inside the Brillouin zone. The low energy part of the spectrum consists of two cones separated by the vector $2\mathbf{Q}$.

the atoms. This spectrum has the property that the valence and conduction band touch at two points in the first Brillouin zone. The low energy physics is then described by particles with conical spectrum (see Fig. 4.2).

It turns out that such an spectrum coincides with the spectrum of two-dimensional Dirac equation for massless particles. Two Dirac cones are centered at two different points (so-called “valleys”) in the Brillouin zone separated by the wave vector $2\mathbf{Q}$. The Dirac fermions have, in fact, eight components corresponding to sublattice, valley and spin indices corresponding to

spinors in 6-dimensional space. Thus one can view the low energy states of graphene as those of 6-dimensional relativistic massless fermions confined to a two-dimensional plane. This fact will play an important role in the subsequent discussion.

Now we are ready to write down the noninteracting Hamiltonian describing states close to the tips of the Dirac cones

$$\begin{aligned}
H_0 &= \sum_k \psi^\dagger(k) \hat{H}_0 \psi(k) \\
\hat{H}_0 &= v \mathbf{k} \vec{\sigma} \otimes \sigma^z \otimes I
\end{aligned}
\tag{4.3}$$

where the Pauli matrices act in the spaces (u, v) , $(Q, -Q)$ and $\sigma = \uparrow, \downarrow$. Here ψ^\dagger, ψ are 8-dimensional spinors made of operators creating and annihilating electrons on different sublattices and in different valleys:

$$\psi^\dagger(k) = (u_\sigma^+(k + K), v_\sigma^+(k + K), v_\sigma^+(k + K'), u_\sigma^+(k + K'))
\tag{4.4}$$

where

$$\mathbf{K} - \mathbf{K}' = 2\mathbf{Q} = \frac{2\pi}{3a} \left(1, \frac{1}{\sqrt{3}} \right) .
\tag{4.5}$$

At larger momenta the spectrum loses rotational symmetry acquiring the so-called trigonal warping [50]. This removes degeneracy between different valleys.

4.1.2 Density Wave Formation and in-plane Magnetic Field

In the present section we discuss the effect of the application of an in-plane magnetic field in a graphene sheet and its relation to density wave formation.

For isolated graphene sheet the Coulomb interaction is rather strong. This induces a possibility of Charge Density Wave (CDW) or Spin Density Wave (SDW) formation. Such intriguing possibility has already been discussed in the literature [51], [52], [53], [54], [55], [56]. The reduced dimensionality of graphene makes a density wave formation even more interesting by enhancing the order parameter fluctuations. As a result the corresponding transition may be converted into a Berezinskii-Kosterlitz-Thouless (BKT) one (if the order parameter has U(1) symmetry) or even shifted to zero temperature, if the corresponding symmetry is non-Abelian.

The CDW order parameter discussed in the papers cited above establishes different population densities on the two sublattices of graphene (we will call them u and v ones) corresponding to a site-centered Density Wave. It was found that without magnetic field order parameters do not form; instead the system is close to Quantum Critical Point [58]. However, a magnetic field perpendicular to the graphene layers may facilitate formation of the CDW [51],[55].

In what follows we suggest that by applying a magnetic field in the graphene plane or a Weiss exchange field [57] one can facilitate a formation of a different order parameter, the one combining all (sublattice, valley and spin) degrees of freedom. This order parameter has $O(4)\times U(1)$ symmetry which may be

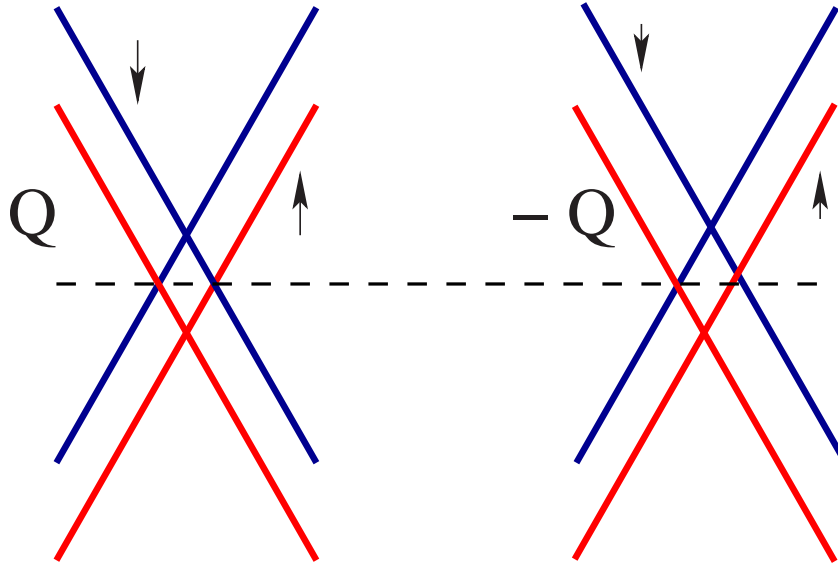


Figure 4.3: Graphene bands split by the in-plane magnetic field.

reduced down to the $O(2)$ one by a slight anisotropy caused by the trigonal warping and the short range spin exchange.

Since magnetic field B lies in the plane, it affects only spin leading to Zeeman splitting of the bands (see Fig. 2). Fermi points become Fermi surfaces with a finite density of states. The density of states at the Fermi surface is easy to obtain,

$$\rho(\epsilon_F) = \frac{k_F}{2\pi v_F} \quad (4.6)$$

where k_F and v_F are Fermi momentum and velocity respectively. This is the arrangement ideal for formation of an exciton insulator.

Application of the magnetic field (B) only introduces a simple additional

term to the non-interacting Hamiltonian (4.3),

$$\begin{aligned}
H_0 &= \sum_k \psi^\dagger(k) \left(\hat{H}_0 + B\hat{b} \right) \psi(k) \\
\hat{H}_0 + B\hat{b} &= v\mathbf{k}\vec{\sigma} \otimes \sigma^z \otimes I + BI \otimes I \otimes \sigma^z
\end{aligned} \tag{4.7}$$

4.2 Mean Field Hamiltonian

The phase transition we are going to study is driven by interactions between quasiparticles. We start then by introducing interactions and treating them using the simplest possible method, namely the mean field theory approach.

The predominant interaction is the Coulomb one:

$$V = \frac{1}{2} \sum_{k,k',q} [\psi^\dagger(\mathbf{k} + \mathbf{q})\psi(\mathbf{k})] \frac{2\pi e^2}{|\mathbf{q}|} [\psi^\dagger(\mathbf{k}' - \mathbf{q})\psi(\mathbf{k}')] \tag{4.8}$$

As we shall demonstrate, the effective interaction at the Fermi surface is significantly screened. At low energies one can neglect frequency and momentum dependence of the interaction and replace $e^2/|\mathbf{k} - \mathbf{k}'|$ in (4.8) by constant V . The estimate of this constant will be given later (see section 4.3); now we will discuss general properties of the order parameter. Decoupling the interaction by the Hubbard-Stratonovich transformation

$$\frac{V}{2} [\psi_a^\dagger \psi_a] [\psi_b^\dagger \psi_b] \rightarrow \frac{\Delta_{ab} \Delta_{ba}}{2V} + \Delta_{ab} \psi_a^\dagger \psi_b \tag{4.9}$$

where indices a, b run from 1 to 8, we arrive to the single-particle mean field

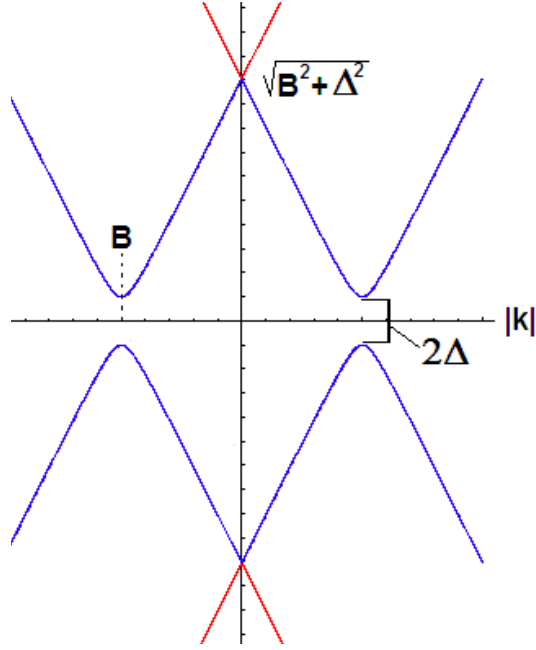


Figure 4.4: The spectrum of quasiparticles below the mean field critical temperature (4.11). A gap opens all around the Fermi surface located at $v|\mathbf{k}| = B$.

Hamiltonian

$$H_{MF} = H_0 + \sum_k \psi_a^\dagger(k) \Delta_{ab} \psi_b(k) \quad (4.10)$$

Diagonalization of (4.10) results in the single-electron spectrum given by

$$E_\pm^2 = \text{Tr}(\Delta^+ \Delta) + v_F^2 (|k| \pm B)^2 \quad (4.11)$$

with a condition that matrix Δ anticommutes with all matrices composing the Hamiltonian (4.3). When the temperature becomes lower than a certain mean field critical temperature (T_{MF}) the order parameter will form, creating a gap in the spectrum of quasiparticles (see Fig. 4.4).

4.2.1 Order Parameter Field

To satisfy invariance of the quasiparticle spectrum (4.11) we find a situation very similar to the one found in the Dirac equation for relativistic quantum mechanics [59]

$$H = \gamma_a p_a + \gamma_0 m \quad (4.12)$$

where, to satisfy the requirement for a relativistic spectrum $E = \pm\sqrt{p^2 + m^2}$, the matrices must have the following properties

$$\{\gamma_a, \gamma_0\} = 0, \quad \{\gamma_a, \gamma_b\} = \delta_{ab}, \quad \gamma_0^2 = I \quad (4.13)$$

In the present situation the matrices have to fulfill similar requirements, namely

$$\{\gamma_{x,y}, \hat{\Delta}\} = 0, \quad \{\gamma_i, \gamma_j\} = \delta_{ij}, \quad \hat{\Delta}^2 = I|\Delta|^2 \quad (4.14)$$

Additionally, the matrix $\hat{\Delta}$ must satisfy

$$\{\hat{b}, \hat{\Delta}\} = 0 \quad (4.15)$$

where $\hat{b} \equiv I \otimes I \otimes \sigma^z$ is the matrix that couples to the in-plane magnetic field.

In summary, $\hat{\Delta}$ is composed of γ matrices of 6-dimensional Dirac equation subject to the additional constraint that they have to anticommute with $I \otimes I \otimes \sigma^z$ which is not a γ matrix. The most general parameterization for a matrix

with such properties is

$$\begin{aligned}
\frac{\hat{\Delta}}{|\Delta|} = & \cos \alpha I \otimes (\cos \phi \sigma^x + \sin \phi \sigma^y) \otimes (\cos \theta \sigma^x + \sin \theta \sigma^y) \\
& + \sin \alpha \cos \beta \sigma^z \otimes \sigma^z \otimes (\cos \theta \sigma^x + \sin \theta \sigma^y) \\
& + \sin \alpha \sin \beta \sigma^z \otimes I \otimes (-\sin \theta \sigma^x + \cos \theta \sigma^y)
\end{aligned} \tag{4.16}$$

Four angles $\alpha, \beta, \phi, \theta$ parameterize the order parameter manifold which, as we will demonstrate, has $O(4) \times U(1)$ symmetry (the trigonal warping, destroying nesting between the Fermi surfaces of electrons from different valleys, selects $\alpha = \pi/2$ and thus lows this symmetry down to $[U(1)]^2$). The short range exchange introduces further anisotropy bringing the symmetry down to $O(2)$. Among other things, this order parameter gives rise to the nonuniform spin density. The part corresponding to on-site Spin Density wave is given by the second term in (4.16):

$$\mathbf{S}_u(\mathbf{r}) \equiv \langle u^+(\mathbf{r}) \vec{\sigma}_\perp u(\mathbf{r}) \rangle \sim \tag{4.17}$$

$$\mathbf{e}_1 \sin \alpha \cos \beta,$$

$$\mathbf{S}_v(\mathbf{r}) \equiv \langle v^+(\mathbf{r}) \vec{\sigma}_\perp v(\mathbf{r}) \rangle$$

$$-\mathbf{e}_1 \sin \alpha \cos \beta,$$

The link-centered SDW originates from the first term:

$$\mathbf{S}_{uv}(\mathbf{r}) \equiv \langle u^+(\mathbf{r}) \vec{\sigma}_\perp v(\mathbf{r}) \rangle \sim \tag{4.18}$$

$$2\mathbf{e}_1 \cos \alpha \cos(2\mathbf{Q}\mathbf{r} + \phi) \tag{4.19}$$

where $\mathbf{e}_{1,2}$ are two mutually perpendicular unit vectors orthogonal to the magnetic field \mathbf{B} (they are parameterized by angle θ). Such SDWs generate Bragg peaks at $\mathbf{q} = 0$ and $\pm 2\mathbf{Q}$ respectively.

4.3 Effective Interaction and Mean Field Critical Temperature

To estimate the magnitude of the spectral gap, we need to estimate the effective interaction on the Fermi surface. The strength of the Coulomb interaction is characterized by the dimensionless parameter $g = \pi e^2 / \hbar v_F$ (in what follows we put $\hbar = 1$) which bare value is rather high ≈ 6.9 . However, as we have mentioned above, the effective interaction at the Fermi surface must be smaller due to the screening. To estimate its magnitude we will follow Son [58], who used a combination of Renormalization Group (RG) theory and $1/N$ approximation, where $N = 4$ is the degeneracy of a single Dirac cone. In this approximation the Coulomb interaction is screened:

$$V(q, \omega_n) = \frac{2\pi e^2}{|q| - 2\pi e^2 N \Pi(\omega_n, q)}, \quad (4.20)$$

where the polarization operator is estimated as

$$\Pi(\omega_n, q) = -\frac{q^2}{\sqrt{v(q)^2 q^2 + \omega_n^2}} \quad (4.21)$$

where $v(q)$ is found from RG equation. The latter equation can be obtained from the equations derived by Gonzalez *et. al.*¹ [62], and Son [58]:

$$N \frac{dg}{d \ln(E_c)} = \frac{8}{\pi^2} \left(g - \pi/2 + \frac{\arccos g}{\sqrt{1-g^2}} \right) \quad (4.22)$$

where $g(E_c) = \pi e^2 N / 4v_F$ and E_c is the running cut-off energy. These equations are obtained for $B = 0$; for B finite the scaling stops at $E_c = B$. As one may expect and as we will confirm below, the gap size is determined by the product of the screened interaction (4.20) at momenta of the order of the Fermi momentum $k_F = B$ and the density of states on the Fermi surface:

$$\bar{g} = \frac{k_F}{2\pi v_F} V(k_F, 0) = \frac{e^2/v_F}{1 + Ne^2/v_F} \quad (4.23)$$

Therefore unless $g(B)$ is smaller than 1, the effective coupling \bar{g} has a universal value $1/N$. From the numerical solution of (4.22) obtained in [62] we see that at bare value $g_0 = 6.9$ the effective coupling $g(B)$ falls below 1 at $N^{-1} \ln(W/B) \approx 4$ (see Fig. 4.5) which corresponds to $B < 10^{-3}\text{K}$. Thus we can conclude that except of very small temperatures and fields one can consider the screened interaction as universal $\bar{g} = 1/N$.

The saddle point conditions for the order parameter are

$$\Delta(k) = T \sum_n \int \frac{d^2p}{(2\pi)^2} V(|\mathbf{k} - \mathbf{p}|) \times \quad (4.24)$$

$$\frac{\Delta(p)[\omega_n^2 + |\Delta(p)|^2 + B^2 + (vp)^2]}{[\omega_n^2 + |\Delta(p)|^2 + B^2 + (vp)^2]^2 - 4(vp)^2 B^2}$$

¹The authors of [62] set $N = 1$. In this case the approximations used in that paper are no longer valid at $g > 1$. For large N the requirement is less stringent: $g/N < 1$.

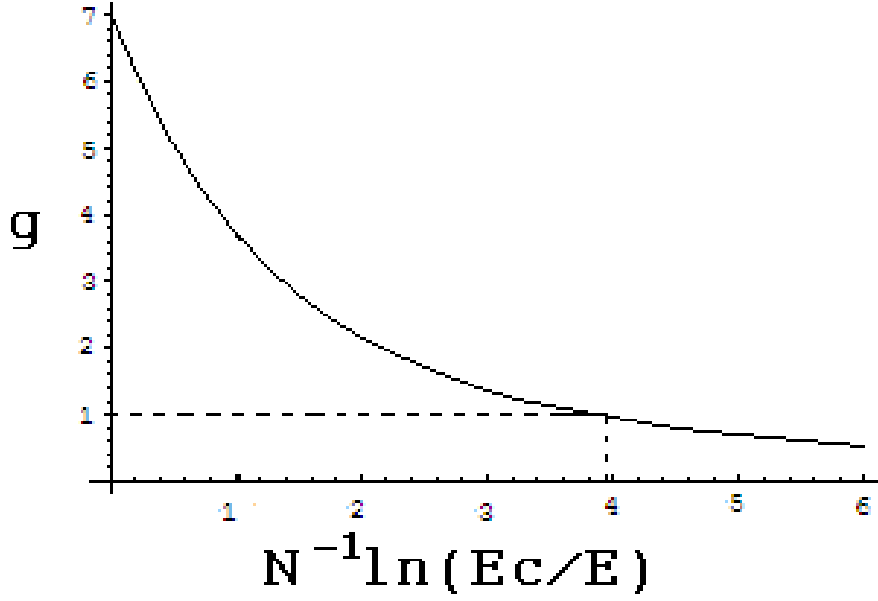


Figure 4.5: Renormalization group flow of g for a bare value of $g_0 \approx 6.9$. g becomes lower than 1 only if $B \leq 10^{-3}K$.

To find the mean field transition temperature we can study the linearized form of this equation. Summing over the Matsubara frequencies and integrating over angles we get the following equation:

$$\Delta(p) = \int \frac{d^2k}{(2\pi)^2} \frac{V(\mathbf{p}-\mathbf{k})}{2} \times \left\{ \frac{\tanh[(v_k|k|+B)\beta/2]}{v_k|k|+B} + \frac{\tanh[(v_k|k|-B)\beta/2]}{(v_k|k|-B)} \right\} \Delta(k) \quad (4.25)$$

Neglecting momentum dependence of V and v_q and taking B as the ultraviolet cut-off we obtain the following estimate for the mean field temperature

$$T_{MF} \approx B \exp(-N) \sim 0.02B \quad (4.26)$$

This formula overestimates T_{MF} for very small fields where the screened interaction is smaller than $1/N$ and probably somewhat underestimates it for higher fields.

For example, for a large but experimentally realistic magnetic field of $B = 20[T]$ the mean field critical temperature would be $T_{MF} \approx 0.3K$.

4.4 Critical Fluctuations

In two space dimensions the mean field temperature T_{MF} just marks a crossover. What happens at lower temperatures is determined by fluctuations and the latter crucially depend on the symmetry of the order parameter. For that reason we decided to derive the Ginzburg-Landau effective action for fluctuations [60], [61].

In order to find the effective action we proceed in the usual way by first introducing an auxiliary field as we already did in section 4.2. Schematically we have

$$Z = \int D\Delta D\Delta^\dagger D\psi D\psi^\dagger e^{S[\psi, \psi^\dagger, \Delta, \Delta^\dagger]} = C \int D\Delta D\Delta^\dagger e^{S_{eff}[\Delta, \Delta^\dagger]} \quad (4.27)$$

where in the right hand side we have integrated out fermions taking advantage of the fact that the action has become quadratic after the transformation. We are left then with an action that depends only on the auxiliary (order parameter) field.

Furthermore, the effective action may be expanded around its mean field (saddle point) solution (Δ_0) to take into account the effect of fluctuations

$(\delta\Delta)$. The contribution of the order parameter fluctuations to the action in the second order is

$$\frac{T}{2} \sum_n \text{Tr} \int \frac{d^2p}{(2\pi)^2} \left(\delta\hat{\Delta}(q)\hat{G}(p+q/2)\delta\hat{\Delta}(-q)\hat{G}(p-q/2) \right)$$

where \hat{G} is the mean field Matsubara Green's function

$$G = \frac{(\omega^2 + B^2 + \hat{\Delta}^2 + p^2 - 2B\bar{\gamma}_\mu p^\mu)(i\omega I - \hat{B} - \hat{\Delta}^a \gamma_a - \gamma_\mu p^\mu)}{[\omega^2 + |\Delta|^2 + (B - |p|)^2][\omega^2 + |\Delta|^2 + (B + |p|)^2]} \quad (4.28)$$

where $\bar{\gamma}_\mu = (\sigma_\mu \otimes \sigma^z \otimes \sigma^z)$ and $\gamma_\mu = (\sigma_\mu \otimes \sigma^z \otimes I)$. At small frequencies $|\omega| \ll B$ we have to take the residue at the corresponding pole which gives

$$G_r = \frac{\left(I - \frac{\bar{\gamma}_\mu p^\mu}{|p|}\right) (i\omega I - \hat{B} - \hat{\Delta}^a \gamma_a - \gamma_\mu p^\mu)}{2[\omega^2 + |\Delta|^2 + (B - |p|)^2]} \quad (4.29)$$

Now one has to use this Green's function to derive the stiffness.

At $T < T_{MF}$ this yields the following Ginzburg-Landau action

$$S = \frac{\rho}{2} \int d\tau d^2x \left[v^{-2} \left(\dot{\theta}^2 + \dot{\mathbf{N}}^2 \right) + (\partial_\mu \theta)^2 + (\partial_\mu \mathbf{N})^2 \right] \quad (4.30)$$

where \mathbf{N} is the four-dimensional unit vector

$$\mathbf{N} = (\sin \alpha \cos \beta, \sin \alpha \sin \beta, \cos \alpha \cos \phi, \cos \alpha \sin \phi) \quad (4.31)$$

and ρ and v are temperature dependent stiffness and velocity of the collective modes. This action describes fluctuations with energies much smaller than

T_{MF} . Its symmetry is $O(4) \times U(1)$, as has been mentioned above. The $U(1)$ phase θ decouples from the rest of the action. Vortices in θ will transform the mean field transition in this sector into the Berezinskii-Kosterlitz-Thouless (BKT) one. When taking into account singular configurations (vortices) the $U(1)$ symmetric part of the action becomes²

$$S_\theta = \frac{1}{2} \int d^2x \left\{ (\partial_\mu \Theta)^2 + \alpha \cos \left(2\pi \sqrt{\frac{\rho}{T}} \Phi \right) \right\} \quad (4.32)$$

where

$$\Theta \equiv \sqrt{\frac{\rho}{T}} \theta \quad (4.33)$$

and Φ is its dual field. The cosine term perturbing the gaussian action becomes relevant when its conformal dimension becomes smaller than the dimensionality of space. That is when

$$\frac{1}{4\pi} \left(2\pi \sqrt{\frac{\rho}{T}} \right)^2 < 2. \quad (4.34)$$

This means that above some critical temperature

$$T_{BKT} = \frac{\pi}{2} \rho \quad (4.35)$$

the additional term representing singular configurations will become relevant and will affect the long distance physics. In other words, at $T < T_{BKT}$ the system is critical and its correlation functions decay as a power law, while at

²For simplicity we keep only the most relevant cosine term in the action.

$T > T_{BKT}$ vortices produce disorder and the system acquires a finite correlation length.

We believe, however, that the corresponding transition temperature will be close to T_{MF} . Indeed, our estimate for the $T = 0$ stiffness yields $\rho(0) = B/6\pi$ (we note in passing that $v(0) = v_F/\sqrt{2}$). We present a detailed calculation of the stiffness in Appendix E. Hence the crude estimate of the BKT temperature

$$T_{BKT} = \frac{\pi}{2}\rho(0) = \frac{B}{12} \quad (4.36)$$

gives the transition temperature less than an order of magnitude larger than T_{MF} . This means that one has to be more subtle and calculate the stiffness at finite T and solve the equation

$$T_{BKT} = \frac{\pi}{2}\rho(T_{BKT}) \quad (4.37)$$

Since close to T_{MF} the stiffness behaves as

$$\rho(T) = \gamma B \left(\frac{T_{MF} - T}{T_{MF}} \right)^2 \quad (4.38)$$

where $\gamma \sim 1/10$, the solution of Eq.(4.37) is

$$\frac{T_{MF} - T_{BKT}}{T_{MF}} \sim \sqrt{\frac{T_{MF}}{\gamma B}} \sim 1 \quad (4.39)$$

Thus the BKT transition occurs relatively closely to the mean field one (see Fig. 4.6).

The orbital part of action (4.30) is the $O(4)$ nonlinear sigma model. At

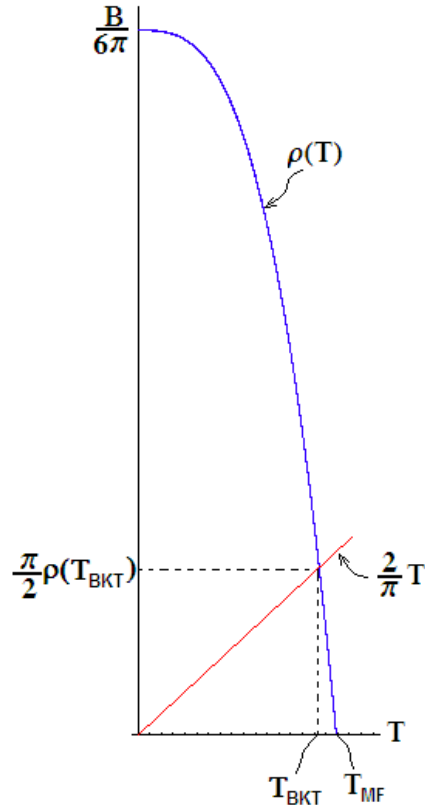


Figure 4.6: The stiffness at zero temperature ($\rho(0)$) is much larger than the mean field critical temperature (T_{MF}) at which the stiffness vanishes. Equation (4.37) is thus solved at a temperature close to T_{MF} .

finite temperatures its stiffness scales to zero and the phase transition occurs only at $T = 0$. At $T \neq 0$ the orbital fluctuations will have a finite correlation length

$$\xi(T) \sim \frac{v_F}{T_{MF}} \exp[2\pi\rho(T)/T] . \quad (4.40)$$

This correlation length will manifest itself in a finite, T -dependent width of the neutron scattering peaks at $\mathbf{q} = 0, \pm 2\mathbf{Q}$.

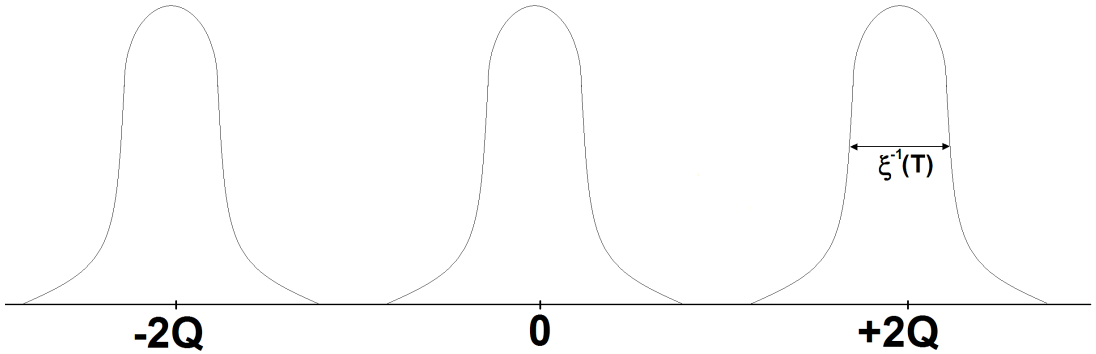


Figure 4.7: Schematic view of expected neutron scattering Bragg peaks. Peaks are located at wavevectors $\mathbf{0}$ and $\pm 2\mathbf{Q}$. The width of the peaks is given by the inverse correlation length of the $O(4)$ non-linear sigma model (4.40).

4.5 Conclusions

A brief summary of our findings is that by applying a strong in-plane magnetic field to a graphene sheet one can facilitate a transition into a state characterized by a single particle gap and strong spin and orbital fluctuations.

The simplest experimental sign of the transition is a rapid drop in electrical conductivity below T_{MF} . This is due to the fact that, as we showed, below this temperature quasiparticle excitations which carry electrical charge will become gapped. Another important experimental signature is the emergence of a broad elastic peaks in the spin structure factors. Since neutrons couple to spin, the cross section from inelastic neutron scattering experiment should show broad peaks similar to the ones shown in Fig. 4.7. The width of the peaks will be determined by the finite correlation length given by orbital fluctuations of \mathbf{N} at any finite temperature. The spin conductivity becomes finite below

certain temperature T_{BKT} (this corresponds to angle θ going critical), but the spin-spin correlation function remain disordered due to the orbital fluctuations.

Chapter 5

General Conclusions

The behavior of materials such as semiconductors and simple metals has been well understood for many years. The main reason for this is that they can be described in terms of free or weakly interacting particle-like excitations (quasiparticles). In this case, fairly straightforward mathematical methods or conventional perturbation theory are enough to explain the phenomena observed in experiments.

There are a large number of materials though, in which the interaction energy is comparable to the kinetic energy and whose properties (e.g. magnetism, high temperature superconductivity, etc.) cannot be explained via the traditional free particle methods. Throughout this thesis we studied some of such strongly correlated systems in low dimensions. As we have seen, reduced dimensionality can be very helpful when dealing with strong correlations.

In Chapters 2 and 3 we studied two different models: quantum Ising chain and crossed spin-1/2 Heisenberg chains respectively, and in each one of them we focused in obtaining correlation functions of physical operators. To ob-

tain correlation functions is of primary importance to be able to describe the physical properties of condensed matter systems. They are proportional to the linear response to experimental probes and often tell us about the properties of the phase the system is in.

The one dimensional Ising model in a transverse field is the simplest model that one can think of to describe magnetic interactions between spins in a solid. Although its direct application to real physical systems is very limited, this model has been widely studied because it illustrates many important properties of condensed matter systems (i.e. second order phase transition). In our work we calculated correlators of the order parameter field. We took advantage of the mapping that exists between the two dimensional classical and the one dimensional quantum Ising model. We basically used exact results for the two point correlator of the classical system [4, 5] as the starting point to obtain the dynamic correlator for the quantum model.

First we worked in the low temperature regime and considered the limit where the gap is much smaller than the bandwidth, allowing for a continuum description of the model. Starting from a form factor representation for the two point correlator obtained in [31] we managed to rewrite it in terms of the partition function of a certain field that lives in a one dimensional space (θ). By using the expression for the correlator we were able to derive a low frequency ($\omega < 2M$) approximation that is valid in the low temperature regime ($T \ll M$) where the soliton density is small. The result contains an imaginary part that reflects the quantum nature of the problem.

In a second study of the same model we considered the high temperature regime ($T \gg J$) where all particles in the band are excited and Lorentz sym-

metry is lost. Since excitations with high momentum are present, processes at the scale of the lattice spacing become relevant and there is no universality. Very little is known about this regime since past research has focused either on finding the ground state properties of the system or in studying it at finite temperature in the universal limit. Our result, valid for very large temperatures and distances is consistent with previously known results. It also confirms that the dynamics of the system is a quantum effect and time dependence only appears when the transverse field is present. Furthermore, it gives the causality relation consistent with the velocity of quasiparticle excitations of the model.

In Chapter 3 we explored a different kind of one dimensional system: the problem of two spin-1/2 Heisenberg chains interacting at one point. It is well known that Heisenberg chains are much more than a mere academic exercise, since they are realized in several quasi one dimensional materials that have a much stronger exchange interaction along a particular direction. In the regime of temperatures larger than the interchain interaction, the chains behave as isolated objects. Furthermore, materials in which only two chains interact with each other (spin ladders) are also known. Our problem of chains interacting at one point corresponds to a particular case of the latter. Admittedly, at the present time we do not know of any physical system that realizes this model, but it is quite possible that such a material would become available in the future.

As we saw, this model is intimately related to the quantum Ising chain. In fact, as it was shown in [47] (see also Appendix D) it can be mapped directly to the problem of four independent critical Ising models with an energy density

perturbation at the origin that is proportional to the interaction among the original Heisenberg chains. Using this equivalence we calculated correlators at the point of the interaction. We showed that the exponents of such correlators are non-universal and are proportional to the interchain interaction.

In Chapter 4 we studied the problem of graphene sheets. This material consists in a two dimensional arrangement of carbon atoms in a honeycomb lattice. Its recent experimental realization sparked an enormous amount of interest in this material. In our work we argued that applying a magnetic field in the direction of the plane of the sheet creates the ideal scenario for excitonic condensation.

As we stressed in the introduction, dimensionality plays an extremely important role in the study of condensed matter systems. Therefore, the methods used when investigating a two dimensional problem are quite different from the ones used for one dimensional systems. For instance a mean field theory (MFT) approximation, while useful in two dimensions, becomes meaningless in one dimension due to enhancement of fluctuations and its results are qualitatively incorrect. We were thus able to use MFT in graphene as a first approximation to obtain an estimate of the critical temperature at which one expects the density wave (DW) order to appear.

To find this critical temperature we also needed an estimate of the magnitude of the effective interaction at the Fermi surface which we derived by using a combination of renormalization group theory and N^{-1} approximation. Since the DW ordering mechanism is made possible by the Zeeman splitting of the bands of electrons with different spin, it is not surprising that the critical temperature we obtained is proportional to the in-plane magnetic field that

produces the splitting.

We also derived the explicit form of the order parameter field that would appear below the critical temperature and showed that it mixes spin, valley and sublattice degrees of freedom. Fluctuations of the order parameter become important in two dimensions and for this reason we derived the corresponding Ginzburg-Landau theory to take them into account. We found that it corresponds to a $O(4) \times U(1)$ symmetric model. In two dimensions, the $O(4)$ part will remain disordered at any finite temperature, whereas vortices in the parameter (θ) of the $U(1)$ symmetry will change the nature of the phase transition to a Berezinskii-Kosterlitz-Thouless one, and will disorder the system at temperatures above some critical temperature T_{BKT} . Using a crude estimate of this temperature we concluded that it has the same order of magnitude as the T_{MF} calculated before.

Appendix A

Matsubara Time Formalism

In order to illustrate the imaginary (Matsubara) time formalism in the simplest way possible we will use a one particle system. Its partition function at finite temperature $T = \beta^{-1}$ may be written in the following way,

$$Z = \text{Tr}\{e^{-\beta H}\} = \int dx \langle x | e^{-\beta H} | x \rangle. \quad (\text{A.1})$$

The exponent can be thought of as the evolution operator in imaginary time, where the time interval is given by the inverse temperature. By dividing β into a large number of infinitesimal slices of size $\epsilon = \beta M^{-1}$ it can be shown that the partition function becomes a path integral

$$Z = \int D[x(\tau)] e^{\int_0^\beta d\tau L_\tau}, \quad (\text{A.2})$$

where L_τ is the Lagrangian of the system after making the change of variables

$$t = -i\tau \quad (\text{A.3})$$

and the integration is over all paths with $x(0) = x(\beta)$.

Correlation functions of operators can be obtained within this same formalism, leading to

$$\langle T\{O(x, \tau_2)O(0, \tau_1)\} \rangle = \frac{1}{Z} \text{Tr}\{e^{-\beta H} T\{O(x, \tau_2)O(0, \tau_1)\}\} \quad (\text{A.4})$$

$$= \frac{1}{Z} \int D[x(\tau)] O(x, \tau_2) O(0, \tau_1) e^{\int_0^\beta d\tau L_\tau} \quad (\text{A.5})$$

where T is the time ordering operator and the evolution is in the imaginary time direction

$$O(x, \tau) = e^{\tau H} O(x, 0) e^{-\tau H}. \quad (\text{A.6})$$

Information about the response of a physical system to experimental probes is contained in real time correlation functions which can be obtained from its imaginary-time version via straightforward analytic continuation.

Appendix B

Transformation of sum (2.67) into a contour integral

In this Appendix we demonstrate how to derive Eq.(2.68). We do it in a manner similar to the one described in [31], namely by transforming the sum (2.67) into a contour integral.

In what follows we will take advantage of the following identities:

$$\begin{aligned} \sinh \frac{\gamma_i + \gamma_j}{2} = & \sqrt{M^2 + \frac{\bar{q}_i^2}{16\lambda}} \sqrt{1 + M^2 + \frac{\bar{q}_j^2}{16\lambda}} \\ & + \sqrt{M^2 + \frac{\bar{q}_j^2}{16\lambda}} \sqrt{1 + M^2 + \frac{\bar{q}_i^2}{16\lambda}} \end{aligned} \quad (\text{B.1})$$

$$\sinh \gamma_j = 2\sqrt{M^2 + \frac{\bar{q}_j^2}{16\lambda}} \sqrt{1 + M^2 + \frac{\bar{q}_j^2}{16\lambda}} \quad (\text{B.2})$$

$$\sinh \frac{\gamma_j}{2} = \sqrt{M^2 + \frac{\bar{q}_j^2}{16\lambda}} = -i \operatorname{sgn}(\Re \alpha_j) \cosh \alpha_j \quad (\text{B.3})$$

$$\cosh \frac{\gamma_j}{2} = \sqrt{1 + M^2 + \frac{\bar{q}_j^2}{16\lambda}} = -i \sinh \alpha_j \quad (\text{B.4})$$

$$\bar{q}_j = -\operatorname{sgn}(\Re \alpha_j) 4i \sqrt{\lambda(\cosh^2 \alpha_j + M^2)} \quad (\text{B.5})$$

with,

$$\alpha_j = i \frac{\pi}{2} \pm \sinh^{-1} \left(\sqrt{M^2 + \frac{\bar{q}_j^2}{16\lambda}} \right) \quad (\text{B.6})$$

In order to be able to simplify notation we define the following,

$$F(\alpha) \equiv -i \frac{[\sinh \alpha - \operatorname{sgn}(\Re \alpha) \cosh \alpha]^{2|r_x|} \{1 + \lambda^{-1} [\sinh \alpha - \operatorname{sgn}(\Re \alpha) \cosh \alpha]^2\}}{\left(e^{\operatorname{sgn}(\Re \alpha) 4\beta \sqrt{\lambda(\cosh^2 \alpha + M^2)}} - 1 \right) \sqrt{\cosh^2 \alpha + M^2}} \quad (\text{B.7})$$

$$TAN^2(\alpha_i, \alpha_j) \equiv \left(\frac{\operatorname{sgn}(\Re \alpha_i) i \sqrt{\cosh^2 \alpha_i + M^2} - \operatorname{sgn}(\Re \alpha_j) i \sqrt{\cosh^2 \alpha_j + M^2}}{\operatorname{sgn}(\Re \alpha_i) \cosh \alpha_i \sinh \alpha_j + \operatorname{sgn}(\Re \alpha_j) \cosh \alpha_j \sinh \alpha_i} \right)^2 \quad (\text{B.8})$$

The discontinuity generated by $\operatorname{sgn}(\Re \alpha)$ arises because we are choosing different values of the square root at each side of the imaginary axis.

The points (B.6) in the plane, are the poles of (B.7). The result (2.67) can

now be written as a multivariable contour integral:

$$g_{2l} \approx \left[\frac{\lambda}{2\pi T} \right]^{2l} \frac{1}{(2l)!} \int_C d\alpha_1 F(\alpha_1) e^{4\tau \operatorname{sgn}(\Re e \alpha_1) \sqrt{\lambda(\cosh^2 \alpha_1 + M^2)}} \dots \quad (\text{B.9})$$

$$\dots \int_C d\alpha_{2l} F(\alpha_{2l}) e^{4\tau \operatorname{sgn}(\Re e \alpha_{2l}) \sqrt{\lambda(\cosh^2 \alpha_{2l} + M^2)}} \prod_{i < j} \operatorname{TANH}^2(\alpha_i, \alpha_j)$$

The integration contour $C = C' + C''$ can be deformed as shown in Fig. B.1. The discontinuity along the imaginary axis is, of course, avoided by the contours.

We can see now that F takes the following form along the contours C_1 (minus sign) and C_6 (plus sign),

$$F(\alpha) = \frac{-i e^{-2|r_x||\alpha|} (1 + \lambda^{-1} e^{-2|\alpha|})}{\left(e^{\pm 4\beta \sqrt{\lambda(\cosh^2 \alpha + M^2)}} - 1 \right) \sqrt{\cosh^2 \alpha + M^2}} \quad (\text{B.10})$$

where α is real. For the contours C_3 (minus sign) and C_4 (plus sign) we have

$$F(\alpha + i\pi) = \frac{-i e^{-2|r_x||\alpha|} (1 + \lambda^{-1} e^{-2|\alpha|})}{\left(e^{\pm 4\beta \sqrt{\lambda(\cosh^2 \alpha + M^2)}} - 1 \right) \sqrt{\cosh^2 \alpha + M^2}} \quad (\text{B.11})$$

We are interested in the situation when $|r_x| \gg 1$, so the exponential in F makes the integrand decrease rapidly with $|\alpha|$. This means that terms in g_{2l} that include integrals along these contours will be at least of order $O(1/|r_x|)$ (smaller) when compared with terms that do not include them. Then, to calculate the leading term it is safe to neglect the part of the integral contained in these contours and keep only the contours C_2 and C_5 . To evaluate the integrals along these contours we define:

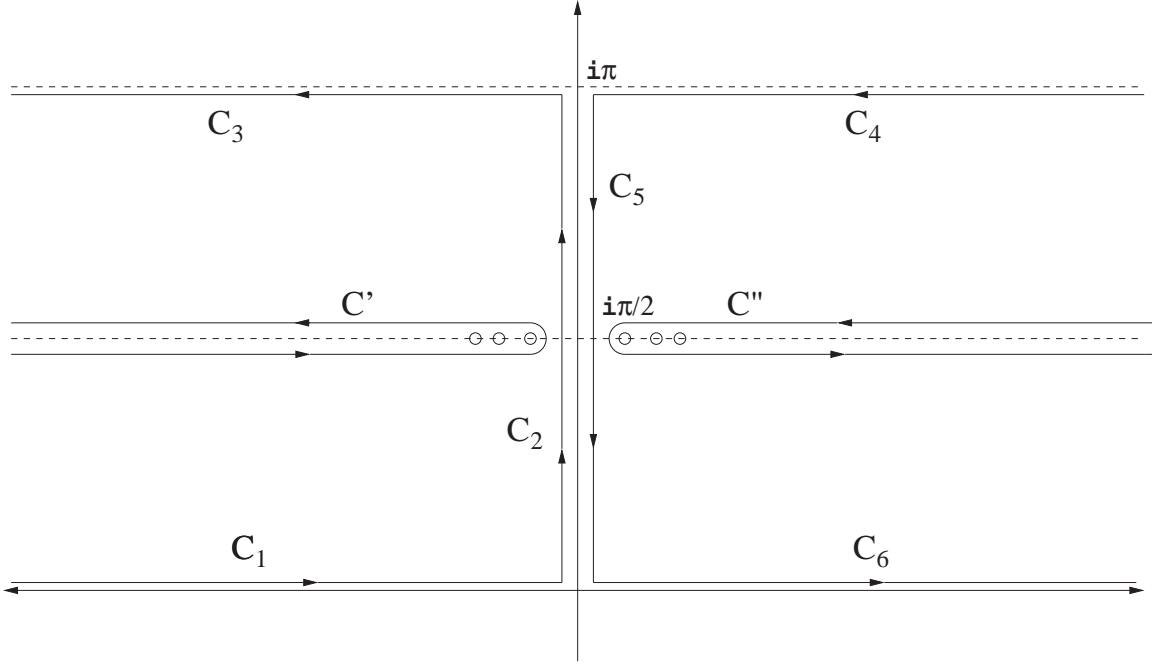


Figure B.1: The figure shows the integration contours in the α plane. The circles are the poles of F at α_j given by (B.6).

$$F^\pm(\alpha) \equiv \frac{-i e^{\mp i2|r_x|\alpha} \left(1 + \lambda^{-1} e^{\mp i2\alpha}\right)}{\left(e^{\pm 4\beta\sqrt{\lambda(\cos^2\alpha + M^2)}} - 1\right) \sqrt{\cos^2\alpha + M^2}} \quad (\text{B.12})$$

$$TAN_\pm^2(\alpha_i, \alpha_j) \equiv \left(\frac{\sqrt{\cos^2\alpha_i + M^2} - \sqrt{\cos^2\alpha_j + M^2}}{\sin(\alpha_i + \alpha_j \mp i2\delta)} \right)^2 \quad (\text{B.13})$$

$$COTAN^2(\alpha_i, \alpha'_j) \equiv \left(\frac{\sqrt{\cos^2\alpha_i + M^2} + \sqrt{\cos^2\alpha'_j + M^2}}{\sin(\alpha_i - \alpha'_j - i2\delta)} \right)^2 \quad (\text{B.14})$$

In equation (B.12) F^+ (F^-) gives the value of F in (B.7) along C_5 (C_2). We

can replace now τ for it to get the following approximation,

$$\begin{aligned}
g_{2l} \approx & \left[\frac{\lambda}{2\pi T} \right]^{2l} \sum_{p=0}^{2l} \frac{1}{p!(2l-p)!} \int_0^\pi \prod_{i=1}^p d\alpha_i F^+(\alpha_i) e^{it 4\sqrt{\lambda(\cos^2 \alpha_i + M^2)}} \quad (\text{B.15}) \\
& \times \prod_{j=1}^{2l-p} d\alpha'_j F^-(\alpha'_j) e^{-it 4\sqrt{\lambda(\cos^2 \alpha'_j + M^2)}} \prod_{i>k} TAN_+^2(\alpha_i, \alpha_k) \\
& \times \prod_{j>m} TAN_-^2(\alpha'_j, \alpha'_m) \prod_{i,j} COTAN^2(\alpha_i, \alpha'_j)
\end{aligned}$$

The demoninator of F^\pm can be easily simplified if we use the obvious approximation for $\beta \ll 1/\lambda$. Let us then write down the result explicitly:

$$\begin{aligned}
g_{2l} \approx & \left[\frac{\sqrt{\lambda}}{8\pi} \right]^{2l} \sum_{p=0}^{2l} \frac{1}{p!(2l-p)!} \int_0^\pi \prod_{i=1}^p d\alpha_i \frac{e^{-i2|r_x|\alpha_i + it 4\sqrt{\lambda(\cos^2 \alpha_i + M^2)}} (1 + \lambda^{-1} e^{-i2\alpha_i})}{\cos^2 \alpha_i + M^2} \\
& \times \prod_{j=1}^{2l-p} d\alpha'_j \frac{e^{i2|r_x|\alpha'_j - it 4\sqrt{\lambda(\cos^2 \alpha'_j + M^2)}} (1 + \lambda^{-1} e^{i2\alpha'_j})}{\cos^2 \alpha'_j + M^2} \\
& \times \prod_{i>k} \left(\frac{\sqrt{\cos^2 \alpha_i + M^2} - \sqrt{\cos^2 \alpha_k + M^2}}{\sin(\alpha_i + \alpha_k - i2\delta)} \right)^2 \\
& \times \prod_{j>m} \left(\frac{\sqrt{\cos^2 \alpha'_j + M^2} - \sqrt{\cos^2 \alpha'_m + M^2}}{\sin(\alpha'_j + \alpha'_m + i2\delta)} \right)^2 \\
& \times \prod_{i,j} \left(\frac{\sqrt{\cos^2 \alpha_i + M^2} + \sqrt{\cos^2 \alpha'_j + M^2}}{\sin(\alpha_i - \alpha'_j - i2\delta)} \right)^2 \quad (\text{B.16})
\end{aligned}$$

We are interested in $|r_x| \gg 1$ and in this case the main contribution to the integral comes from regions around the divergencies. There are divergencies that originate from $\alpha_i - \alpha'_j = 0, \pm\pi$. Let us take into account only the terms in g_{2l} which are maximally singular. This maximal singularity occurs when

$p = l$ and in regions where every α pairs with an α' in order to approach a singularity. There are $2^l l!$ of these regions. Finally we get the following approximation,

$$\begin{aligned}
g_{2l} &\approx \frac{1}{l!} \left(\frac{\lambda}{32\pi^2} \int_0^\pi d\alpha \int_{-\infty}^\infty d\epsilon \frac{e^{-i4|r_x|\epsilon + 4it\sqrt{\lambda}(\sqrt{\cos^2 \alpha + M^2} - \sqrt{\cos^2(\alpha - 2\epsilon) + M^2})}}{(\epsilon - i0)^2} \times \right. \\
&\quad \left. \frac{(1 + \lambda^{-1}e^{-i2\alpha})(1 + \lambda^{-1}e^{i2(\alpha - 2\epsilon)}) \left(\sqrt{\cos^2 \alpha + M^2} + \sqrt{\cos^2(\alpha - 2\epsilon) + M^2} \right)^2}{(\cos^2 \alpha + M^2)(\cos^2(\alpha - 2\epsilon) + M^2)} \right)^l \\
&= \frac{1}{l!} \left[-\frac{\lambda}{\pi} \int_0^\pi d\alpha \frac{(1 + \lambda^{-1}e^{-i2\alpha})(1 + \lambda^{-1}e^{i2\alpha})}{\cos^2 \alpha + M^2} \left(\frac{2t\sqrt{\lambda} \sin \alpha \cos \alpha}{\sqrt{\cos^2 \alpha + M^2}} - |r_x| \right) \times \right. \\
&\quad \left. \theta \left(\frac{2t\sqrt{\lambda} \sin \alpha \cos \alpha}{\sqrt{\cos^2 \alpha + M^2}} - |r_x| \right) \right]^l \\
&\equiv \frac{1}{l!} [-R(t, |r_x|, \lambda)]^l \tag{B.17}
\end{aligned}$$

where

$$R \equiv \frac{4}{\pi} \int_0^\pi d\alpha \left(\frac{2t\sqrt{\lambda} \sin \alpha \cos \alpha}{\sqrt{\cos^2 \alpha + M^2}} - |r_x| \right) \theta \left(\frac{2t\sqrt{\lambda} \sin \alpha \cos \alpha}{\sqrt{\cos^2 \alpha + M^2}} - |r_x| \right) \tag{B.18}$$

And considering that,

$$\Lambda^{-1} \approx \log \frac{T}{\lambda} \tag{B.19}$$

we get the final result for the dynamical (real time) correlation function in the form of (2.68).

Appendix C

Bosonization of the Heisenberg chain

The low energy physics of the one dimensional spin-1/2 Heisenberg chain can be described in terms of bosonic degrees of freedom via the so called, Bosonization technique. This method has proven to be very powerful and has been used to understand various one dimensional models. For more details on the Bosonization procedure the reader is referred to books [46],[63],[64] that describe the subject extensively.

For simplicity we will start by showing how the more general anisotropic (XXZ) chain is Bosonized. The Hamiltonian of the XXZ chain is

$$H_{XXZ} = J \sum_i (S_i^x S_{i+1}^x + S_i^y S_{i+1}^y + \Delta S_i^x S_{i+1}^y) \quad (\text{C.1})$$

where the spin-1/2 operators satisfy the usual commutation relations

$$[S^\alpha, S^\beta] = i\epsilon^{\alpha\beta\gamma} S^\gamma \quad (\text{C.2})$$

and $|\Delta| < 1$ is the anisotropy parameter.

In one dimension this problem can be mapped into the problem of interacting spinless fermions via the well known Jordan-Wigner transformation

$$\begin{aligned} S_i^+ &= c_i^\dagger e^{i\pi \sum_{j<i} c_j^\dagger c_j} \\ S_i^- &= c_i e^{-i\pi \sum_{j<i} c_j^\dagger c_j} \\ S^z &= c_i^\dagger c_i - 1/2 \end{aligned} \quad (\text{C.3})$$

In this new fermionic basis the Hamiltonian becomes

$$H_{XXZ} = \frac{J}{2} \sum_i c_i^\dagger c_{i+1} + c_{i+1}^\dagger c_i + 2\Delta (c_i^\dagger c_i - 1/2)(c_{i+1}^\dagger c_{i+1} - 1/2) \quad (\text{C.4})$$

The limit $\Delta = 0$ of this Hamiltonian can be easily diagonalized obtaining the following spectrum for fermionic excitations,

$$\epsilon(p) = J \cos(pa) \quad (\text{C.5})$$

The ground state of such a system corresponds to the spectrum filled to $p_F = \pi/2$. Since we are interested in the low energy properties of the system, we can truncate the spectrum around the Fermi points. As a result we are left

with excitations that have linear spectrum in the vicinity of $\pm p_F$

$$R(x) = \sum_{p=-\Lambda}^{\Lambda} c_{p+p_F} e^{i(p+p_F)x}, \quad L(x) = \sum_{p=-\Lambda}^{\Lambda} c_{p-p_F} e^{i(p-p_F)x} \quad (\text{C.6})$$

where $\Lambda \ll p_F$ and their spectrum is

$$\epsilon_{R,L}(p) = \pm v_F p, \quad v_F = J a$$

The resulting low energy Hamiltonian of the XY chain ($\Delta = 0$) is

$$H_{XY} = i v_F \int dx (R^\dagger \partial_x R - L^\dagger \partial_x L) \quad (\text{C.7})$$

which can be directly mapped onto the free boson model

$$H = \frac{v_F}{2} \int dx (\Pi^2 + (\partial_x \Phi)^2). \quad (\text{C.8})$$

There is also the following equivalence between fermionic and bosonic operators

$$R(x) \sim \frac{1}{\sqrt{2\pi a}} e^{i\sqrt{4\pi}\varphi_+(x)}, \quad L(x) \sim \frac{1}{\sqrt{2\pi a}} e^{-i\sqrt{4\pi}\varphi_-(x)} \quad (\text{C.9})$$

where

$$\varphi_\pm = \frac{\Phi \pm \Theta}{2} \quad (\text{C.10})$$

with Θ being the dual field of Φ .

We can now write the original spin operators in terms of the bosonic field

operators

$$S^z(x) = \frac{1}{\sqrt{\pi}} \partial_x \Phi(x) - \lambda (-1)^n \sin \sqrt{4\pi} \Phi(x) \quad (\text{C.11})$$

$$S^\pm(x) = \lambda' (-1)^n e^{\pm i \sqrt{\pi} \Theta(x)} \quad (\text{C.12})$$

where λ and λ' depend on Δ .

At $\Delta \ll 1$ the anisotropy term can be added by using the expression for S^z in terms of bosonic operators

$$H_{XXZ} = \frac{v_F}{2} \int dx \left(\Pi^2 + (1 + 4\Delta/\pi) (\partial_x \Phi)^2 + \frac{2\Delta}{(\pi a)^2} \cos(\sqrt{16\pi} \Phi) \right) \quad (\text{C.13})$$

A simple RG analysis shows that the last term is irrelevant and may be ignored when considering the low energy physics, leaving only the Gaussian part. Furthermore, it can be shown that such a description is valid for any anisotropy inside the critical region $-1 < \Delta \leq 1$ leaving a low energy Hamiltonian of the form

$$H_{XXZ} = \frac{u}{2} \int dx \left(K \Pi^2 + \frac{1}{K} (\partial_x \Phi)^2 \right) \quad (\text{C.14})$$

where the parameters can be obtained from the exact Bethe ansatz solution of (C.1)

$$K = \frac{\pi}{2(\pi - \cos^{-1} \Delta)}, \quad u = \frac{\pi v_F}{2} \frac{\sqrt{1 - \Delta^2}}{\cos^{-1} \Delta} \quad (\text{C.15})$$

It is easy to see then that the $SU(2)$ symmetric point ($\Delta = 1$) corresponds

to Luttinger liquid parameters

$$K = \frac{1}{2}, \quad u = \frac{\pi v_F}{2} . \quad (\text{C.16})$$

Appendix D

Transformation of two Heisenberg chains into Majorana fermions

There is a beautiful equivalence between the problem of two coupled spin-1/2 Heisenberg chains and the one of four independent Ising chains in a transverse magnetic field. Since this equivalence is exploited in Chapter 3 we will explain here the steps missing in the main text. We will outline only the basic steps in the derivation and the reader interested in further details is referred to [47] (see also [63] for a more detailed description).

We begin by writing down the bosonized version (C) of the Hamiltonian of two coupled spin-1/2 Heisenberg chains (3.1). All our derivation will be done for the special case of one point interaction between the chains since this is

the problem Chapter 3 addresses. The Hamiltonian of the system is

$$H = H_0 + H_{int} \quad (\text{D.1})$$

where H_0 corresponds to the two independent chains

$$H_0 = \sum_i \frac{v_F}{2} \int dx (\Pi_i^2 + (\partial_x \phi_i)^2) \quad (\text{D.2})$$

where i labels the chains. The second term (H_{int}) corresponds to the most relevant interaction between the chains

$$H_{int} = \frac{g\lambda^2}{2\pi^2} [\cos \sqrt{2\pi}(\phi_1 - \phi_2) - \cos \sqrt{2\pi}(\phi_1 + \phi_2) + 2 \cos \sqrt{2\pi}(\theta_1 - \theta_2)] |_{x=0} \quad (\text{D.3})$$

where $g = J_\perp a$. Introducing the new fields

$$\phi_\pm = \frac{\phi_1 \pm \phi_2}{2}, \quad \theta_\pm = \frac{\theta_1 \pm \theta_2}{2} \quad (\text{D.4})$$

the Hamiltonian can be written as two completely independent parts

$$H = H_+ + H_- \quad (\text{D.5})$$

where

$$H_+ = \frac{v_F}{2} \int dx (\Pi_+^2 + (\partial_x \phi_+)^2) - \frac{m}{\pi} \cos \sqrt{4\pi} \phi_+(x=0) \quad (\text{D.6})$$

$$H_- = \frac{v_F}{2} \int dx (\Pi_-^2 + (\partial_x \phi_-)^2) + \frac{m}{\pi} \cos \sqrt{4\pi} \phi_-(x=0) + \frac{2m}{\pi} \cos \sqrt{4\pi} \theta_-(x=0)$$

where $m = g\lambda^2/2\pi$. The problem can then be rewritten in terms of the following fermionic degrees of freedom (re-fermionization)

$$\psi_+^{R,L} = \frac{1}{\sqrt{2\pi a}} e^{\pm i\sqrt{4\pi}\phi_+^{R,L}} \quad (\text{D.7})$$

and similarly for ϕ_- . Furthermore, each one of this fermions can be decomposed into two Majorana (real) fermions

$$\psi_{\pm}^{R,L} = \xi_1^{\pm;R,L} + i\xi_2^{\pm;R,L} \quad (\text{D.8})$$

in terms of which we can rewrite

$$H_+ = H_m[\xi_1^+] + H_m[\xi_2^+] \quad (\text{D.9})$$

$$H_- = H_m[\xi_1^-] + H_{-3m}[\xi_2^-] \quad (\text{D.10})$$

where

$$H_m[\xi_1] = i \int dx \frac{v_F}{2} (\xi^L \partial_x \xi^L - \xi^R \partial_x \xi^R) - im\delta(x)\xi^R \xi^L \quad (\text{D.11})$$

Finally we obtain the desired result that the original Hamiltonian (D.1) can be reformulated as a problem of four independent pairs of Majorana fermions

$$H = \sum_{a=0}^4 H_{m_a} \quad (\text{D.12})$$

where $m_i = m$ ($i = 1, 2, 3$); $m_0 = -3m$ and the Hamiltonian is then equivalent to (3.3).

A simple inverse Jordan-Wigner transformation (C.3) permits the reformulation of this problem in terms of spin degrees freedom. As a result one obtains that the problem of two spin-1/2 Heisenberg chains can be mapped into the problem of four independent Ising chains in a transverse magnetic field (3.5).

Appendix E

Calculation of Stiffness (ρ) for Ginzburg-Landau Theory (4.30)

As we showed in section 4.4, to analyze the effect of critical fluctuations we have to obtain the contribution of the order parameter fluctuations to the action. It was shown that to the second order it is given by

$$\frac{1}{2} \text{Tr} \int \frac{d^3 p}{(2\pi)^3} \left(\delta \hat{Q}(q) \hat{G}_r(p + q/2) \delta \hat{Q}(-q) \hat{G}_r(p - q/2) \right) \quad (\text{E.1})$$

To obtain the stiffness we have to calculate the q^2 term in the expansion for the polarization loop. This term gives the following contribution to (E.1):

$$\text{Tr} \int \frac{d^2 p d\omega}{(2\pi)^3} \left\{ \frac{\partial_\mu Q \hat{\pi} \partial_\mu Q \hat{\pi}}{8[\omega^2 + \epsilon^2(p)]^2} - \frac{\partial_\mu Q \hat{\pi}(i\omega - \hat{P}) \partial_\mu Q \hat{\pi}(i\omega - \hat{P})}{[\omega^2 + \epsilon^2(p)]^4} \left(\frac{\omega^2 + \epsilon^2}{4} - \frac{(B - p)^2}{2} \right) \right\} \quad (\text{E.2})$$

where

$$\epsilon^2 = (p - B)^2 + Q^2, \quad \hat{\pi} = \frac{1}{2} \left(I - \frac{\bar{\gamma}_\mu p^\mu}{|p|} \right), \quad \hat{P} = \hat{B} + Q^a \gamma_a + \gamma_\mu p^\mu \quad (\text{E.3})$$

Although in principle the stiffness is a temperature dependent parameter ($\rho(T)$), for simplicity we perform the calculation only for $T = 0$. Taking into account that

$$[\hat{\pi}, \hat{B}] = 0, \quad \pi^2 = \pi, \quad [\partial_\mu Q, \hat{\pi}] = 0, \quad Q\delta Q = 0 \quad (\text{E.4})$$

and

$$\hat{\pi}(p)(\hat{B} + \gamma_\mu p^\mu) = \hat{\pi}(p)\hat{b}(B - p) \quad (\text{E.5})$$

where $\hat{b} = (I \otimes I \otimes \sigma^z)$ we arrive to the expression

$$\frac{1}{4} \rho \text{Tr} \langle \partial_\mu Q \hat{\pi} \partial_\mu Q \rangle = \frac{1}{8} \rho \text{Tr} (\partial_\mu Q \partial_\mu Q) \quad (\text{E.6})$$

where $\langle \dots \rangle$ means angle average and

$$\begin{aligned} \rho &= 4 \int \frac{d\omega d^2 p}{(2\pi)^3} \left[\frac{1}{8(\omega^2 + \epsilon^2)^2} + \frac{(\omega^2 + (B - p)^2)(\omega^2 - (B - p)^2 + Q^2)}{4(\omega^2 + \epsilon^2)^4} \right] \\ &= \frac{B}{6\pi Q^2} \end{aligned} \quad (\text{E.7})$$

Now we have to take into account that

$$\partial_\mu Q = \partial_\mu n_1 \gamma_1 + \partial_\mu n_2 \gamma_2 + \partial_\mu n_3 \gamma_3$$

$$\begin{aligned}
& + n_1[\partial_\mu\phi(I \otimes (-\sin\phi\sigma^x + \cos\phi\sigma^y) \otimes (\cos\theta\sigma^x + \sin\theta\sigma^y)) \\
& + \partial_\mu\theta(I \otimes (\cos\phi\sigma^x + \sin\phi\sigma^y) \otimes (\cos\theta\sigma^y - \sin\theta\sigma^x))] \\
& + n_2\partial_\mu\theta(\sigma^z \otimes \sigma^z \otimes (\cos\theta\sigma^y - \sin\theta\sigma^x)) \\
& + n_3\partial_\mu\theta(\sigma^z \otimes I \otimes (\cos\theta\sigma^x + \sin\theta\sigma^y))
\end{aligned} \tag{E.8}$$

where $n_1^2 + n_2^2 + n_3^2 = 1$ and γ_i matrices are

$$\begin{aligned}
\gamma_1 &= (I \otimes (\cos\phi\sigma^x + \sin\phi\sigma^y) \otimes (\cos\theta\sigma^x + \sin\theta\sigma^y)), \\
\gamma_2 &= (\sigma^z \otimes \sigma^z \otimes (\cos\theta\sigma^x + \sin\theta\sigma^y)), \\
\gamma_3 &= (\sigma^z \otimes I \otimes (\cos\theta\sigma^y - \sin\theta\sigma^x))
\end{aligned} \tag{E.9}$$

Thus well below the mean field transition temperature the Ginzburg-Landau free energy has the following form:

$$F/T = \frac{B}{12\pi T} \int d^2x \mathcal{E} \tag{E.10}$$

where

$$\mathcal{E} = (\partial_\mu\alpha)^2 + \sin^2\alpha(\partial_\mu\beta)^2 + \cos^2\alpha(\partial_\mu\phi)^2 + (\partial_\mu\theta)^2 \tag{E.11}$$

and the parameters are defined as in (4.16). The free energy can then be rewritten in terms of an $O(4)$ nonlinear sigma model plus the action of a $U(1)$ symmetric model (see Eqn. 4.30).

Comparing E.10 and 4.30 one can finally obtain the result for the zero

temperature stiffness

$$\rho(T = 0) = \frac{B}{6\pi}. \quad (\text{E.12})$$

Bibliography

- [1] H. Bethe, Z. für Phys., **71**, 205 (1931).
- [2] D. A. Tennant, R. A. Cowley, S. E. Nagler and A. M. Tsvelik, Phys. Rev. B, **52**, 13368 (1995).
- [3] M. Takano, Z. Hiroi, M. Azuma and Y. Bando, J. Solid State Chem., **95**, 230 (1991).
- [4] A. I. Bugrij, in *Integrable Structures of Exactly Solvable Two-Dimensional Models of Quantum Field Theory*, eds. S. Pakuliak and G. von Gehlen, Kluwer Academic, NATO Series, hep-th/0107117
- [5] A. I. Bugrij and O. Lisovyy, JETP **94** (2002) 1140.
- [6] A. I. Bugrij and O. O. Lisovyy, Theoretical and Mathematical Physics, **140** (1), 987 (2004).
- [7] K. von Klitzing, G. Dorda and M. Pepper, Phys. Rev. **45**, 494 (1980).
- [8] D. C. Tsui, H. L. Stormer and A. C. Gossard, Phys. Rev. Lett. **48**, 1559 (1982).
- [9] R. E. Peierls, Ann. I. H. Poincare **5**, 177 (1935).

- [10] L. D. Landau, Phys. Z. Sowjetunion **11**, 27 (1937).
- [11] J. G. Bednorz and K. A. Müller, Z. Phys. B: Cond. Matter **64**, 189 (1986).
- [12] K. S. Novoselov, A. K. Geim, S. V. Morozov, D. Jiang, Y. Zhang, S. V. Dubonos, I. V. Grigorieva and A. A. Firsov, Science **306**, 666 (2004).
- [13] K. S. Novoselov, D. Jiang, F. Schedin, T. J. Booth, V. V. Khotkevich, S. V. Morozov, A. K. Geim, Proc. Natl. Acad. Sci. USA **102**, 10451 (2005).
- [14] B. M. McCoy and T. T. Wu, *The Two Dimensional Ising Model*, (Harvard University Press, 1973).
- [15] One can find a summary of the early results on the Ising model in J. H. Perk, H. W. Capel, G. R. W. Quispel and F. W. Nijhoff, Physica A **123**, 1 (1984).
- [16] S. Sachdev, *Quantum Phase Transitions*, (Cambridge University Press, 1999).
- [17] E. Ising, Z. Physik **31** 253 (1925).
- [18] P. E. Hansen, T. Johansson and R. Nevald, Phys. Rev. B, **12**, 5315 (1975).
- [19] P. Jordan and E. Wigner, Z. Phys. **47**, 631 (1928).
- [20] P. Pfeuty, Ann. Phys., **57**, 79 (1970).
- [21] E. Fradkin and L. Susskind, Phys. Rev. D, **17**, 2637 (1978).
- [22] M. Karowski and P. Weisz, Nucl. Phys. B **139**, 445 (1978).
- [23] B. Berg, M. Karowski and P. Weisz, Phys. Rev. D **19**, 2477 (1979).

- [24] F. A. Smirnov, *Form Factors in Completely Integrable Models of Quantum Field Theory*, Advanced Series in Mathematical Physics, Vol. 14, World Scientific, Singapore (1992).
- [25] A. Leclair, F. Lesage, S. Sachdev and H. Saleur, Nucl. Phys. B, **482**, 579 (1996).
- [26] A. R. Its, A. G. Izergin, V. E. Korepin and N. A. Slavnov, Phys. Rev. Lett. **70** (1993) 1704.
- [27] The most complete summary of this approach can be found in V.E. Korepin, N. M. Bogoliubov, A. G. Izergin, *Quantum Inverse Scattering Method and Correlation Functions*, Cambridge University Press (1993) Cambridge.
- [28] S. Sachdev and A. P. Young, Phys. Rev. Lett. **78**, 2220 (1997).
- [29] A. Rapp and G. Zarand, *Dynamical Correlations and Quantum Phase Transitions in the Quantum Potts Model*, cond-mat/0507390.
- [30] K. Damle and S. Sachdev, Phys. Rev. Lett. **95**, 187201 (2005).
- [31] B. L. Altshuler, R. M. Konik and A. M. Tsvelik, Nucl. Phys. B**739**, 311 (2006).
- [32] R. J. Kubo, Phys. Soc. Japan, **12**, 570 (1957).
- [33] B. M. McCoy, J. H. H. Perk and R. E. Shrock, Nucl. Phys. B**220**, 269 (1983).
- [34] V. E. Korepin, Comm. Math. Phys. **113**, 177 (1987).

- [35] V. E. Korepin and N. A. Slavnov, J. Phys. **A31**, 9283 (1998).
- [36] V. E. Korepin and T. Oota, J. Phys. **A31**, L371 (1998).
- [37] Lukyanov S., Comm. Math. Phys. **167**, 183 (1995).
- [38] M. Mohan, Phys. Rev. **B21**, 1264 (1980); **B23**, 433 (1981).
- [39] *Table of Integrals, Series, and Products*, I. S. Gradshteyn and I. M. Ryzhik, Academic Press, Inc. (London) (1979).
- [40] A. M. Tsvetik and P. B. Wiegmann, Adv. Phys. **32**, 331 (1983).
- [41] P. Schlottmann, Phys. Rep. **181**, 1 (1989).
- [42] P. Fendley, A. W. W. Ludwig and H. Saleur, Phys.Rev. Lett. **74**, 3005 (1995).
- [43] A. M. Chang, Rev. Mod. Phys. **74**, 1449 (2003).
- [44] P. Nozieres and A. Blandin, J. de Physique **41**, 193 (1980).
- [45] A. Luther and I. Peschel, Phys. Rev. B **12**, 3908 (1975).
- [46] A. O. Gogolin, A. A. Nersesyan and A. M. Tsvetik, *Bosonization in Strongly Correlated Systems*, Cambridge University Press, 1999.
- [47] D. G. Shelton, A. A. Nersesyan and A. M. Tsvetik, Phys. Rev. B **53**, 8521 (1996).
- [48] A. A. Nersesyan and A. M. Tsvetik, Phys. Rev. Lett. **78**, 3939 (1997).
- [49] P. Di Francesco, P. Mathieu and D. Senechal, *Conformal Field Theory* (Springer, New York, 1997).

- [50] R. Saito, G. Dresselhaus and M. S. Dresselhaus, Phys. Rev. B **61**, 2981 (2000).
- [51] D. V. Khveshchenko, Phys. Rev. Lett. **87**, 246802 (2001).
- [52] D. V. Khveshchenko, Phys. Rev. Lett. **87**, 206401 (2001).
- [53] D. V. Khveshchenko and H. Leal, Nucl. Phys. B **687**, 323 (2004).
- [54] D. V. Khveshchenko and W. F. Shively, Phys. Rev. B **73**, 115104 (2006).
- [55] E. V. Gorbar, V. P. Gusynin, V. A. Miransky and I. A. Shovkovy, Phys. Rev. B **66**, 045108 (2002).
- [56] I. F. Herbut, cond-mat/0606195.
- [57] I. Zaliznyak, private communication.
- [58] D. T. Son, cond-mat/0701501.
- [59] R. Shankar, *Principles of Quantum Mechanics*, (Springer, 1994)
- [60] V. L. Ginzburg and L. D. Landau, Zh. Eksp. Teor. Fiz. **20**, 1064 (1950).
- [61] L. D. Landau and E. M. Lifshitz, *Statistical Physics, Part I*, (Pergamon Press, 1980)
- [62] J. Gonzalez, F. Guinea and M. A. H. Vozmediano, Phys. Rev. B **59**, R2474 (1999).
- [63] A. M. Tsvelik, *Quantum Field Theory in Condensed Matter Physics*, (Cambridge University Press, 2003)

- [64] T. Giamarchi, *Quantum Physics in One Dimension* (Oxford University Press, 2004)